GeoArabia, 2011, v. 16, no. 2, p. 17-42
Gulf PetroLink, Bahrain

2-D Basin modeling study of petroleum systems in the Levantine Basin, Eastern Mediterranean

Lisa Marlow, Kristijan Kornpihl and Christopher G. St. C. Kendall

ABSTRACT

The Levantine Basin has proven hydrocarbons, yet it is still a frontier basin. There have been significant oil and gas discoveries offshore the Nile Delta, e.g. several Pliocene gas plays and the Mango Well with ca. 10,000 bbls/day in Lower Cretaceous rocks and recently, Noble Energy discovered two gas "giants" (> 5 TCF and one estimated at 16 TFC) one of which is in a pre-Messinian strata in ca. 1,700 m (5,577 ft) water depth. Regional two-dimensional (2-D) petroleum system modeling suggests that source rocks generated hydrocarbons throughout the basin. This paper provides insight into the petroleum systems of the Levantine Basin using well and 2-D seismic data interpretations and PetroMod2D. Tectonics followed the general progression of the opening and closing of the Neo-Tethys Ocean: rift-extension, passive margin, and compression. The stratal package is up to 15 km thick and consists of mixed siliciclastic-carbonate-evaporite facies. Five potential source rock intervals (Triassic – Paleocene) are suggested. Kerogen in the older source rocks is fully transformed, whereas the younger source rocks are less mature. There are several potential reservoir and seal rocks. The model suggests that oil and gas accumulations exist in both structural and stratigraphic traps throughout the basin.

INTRODUCTION

Although the Levantine Basin has proven hydrocarbons, further examination of the tectono-stratigraphic and thermal history of the basin and their affect on the petroleum systems is required to lower exploration risk. This study combined tectono-stratigraphic interpretations developed using well and 2-D seismic data (TGS-NOPEC Geophysical Company) (Figure 1) and 2-D petroleum system modeling (PetroMod2D®) to gain insight into the petroleum systems of the Levantine Basin. Results of the 2-D models indicate that the tectono-stratigraphic, burial, and thermal history favor generation, migration and accumulation of petroleum throughout the Levantine Basin.

The Levantine Basin is a wrench basin bounded by the Cyprus Arc and Eratosthenes Seamount to the north and west, and the African and Arabian plates to the south and east (Figure 1a). For most of its existence it was part of the larger Neo-Tethyan Basin (Figure 1b) (Robertson, 1998; Walley, 1998; Stampfli et al., 2001; Ziegler et al., 2001; Garfunkel, 2004). There are many tectono-stratigraphic similarities between the Levantine Basin and other regions that evolved along the southern Neo-Tethyan margin. However, while these other regions have established petroleum reserves, the Levantine Basin is underexplored. Most exploration in the basin has been near the eastern and southern continental margin bordering the Levantine Basin (Aal et al., 2000; Dolson et al., 2001, 2005; Feinstein et al., 2002; Horscroft and Peck, 2005; Gardosh et al., 2006 and 2008; Peck, 2008; Roberts and Peace, 2007; Semb, 2009). The exploration has resulted in the discovery of numerous noncommercial hydrocarbon shows in wells along the eastern and southern modern continental shelf, including the Mango Well, which tested an estimated 10,000 bbls/day in Lower Cretaceous sands, and several gas plays in Pliocene siliciclastics in the Nile Delta region (Figure 1) (Peck, 2008). There has been very little exploration in the deeper part of the basin.

However, recently the Tamar, and Dalit, and Leviathan wells were drilled in the deeper part (> 1,000 m water depth (3,280 ft)) (Figure 1) and they resulted in major discoveries. The Tamar "giant" gas discovery has an estimated > 5 TCF gas in a sub-Messinian salt structural trap (Early Miocene) and the Leviathan discovery, which is near Tamar, has an estimated 16 TCF of gas (Ben-David, 2010) confirms significant petroleum accumulations in the Levantine Basin (Offshore Engineer Staff, 2009; Scandinavian Oil and Gas Magazine Staff, 2009). These discoveries have led to changes in the USGS's estimate of the Levantine Basin province undiscovered reserves from zero to 122 TCF gas and 1.7 Bbbl oil (Offshore Staff, 2010).

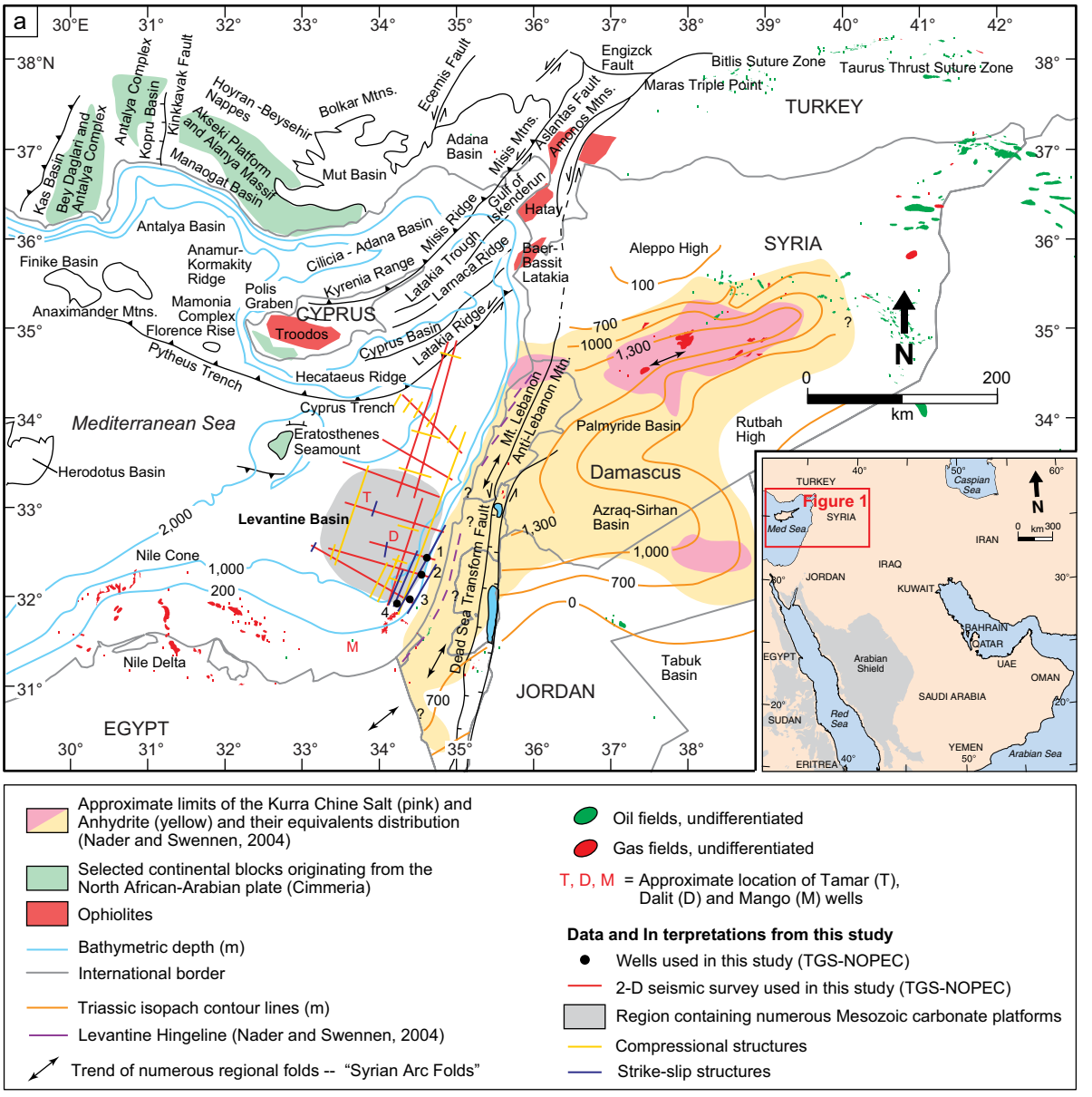

Figure 1: Levantine Basin, regional features and paleogeography of the southern Neo-Tethyan Margin.

(a) Regional data and interpretations from this study: delineation of Kurra Chine salt and related facies (Nader and Swennen, 2004); rafted continental blocks (Robertson, 1998; Garfunkel, 1998, 2004; Stampfli et al., 2001); ophiolites (Robertson, 2002); bathymetric depth; Triassic isopach contour lines (Nader and Swennen, 2004); Levantine Hingeline, Syrian Arc folds and faults (Walley 1998; Beydoun, 1999; Mouty, 2000; Sawaf et al., 2001; Mart et al., 2005); oil and gas fields; general location of Tamar (T), Dalit (D), and Mango (M) wells; data set for this study - 4 wells (depth range 3,210–5,707 m (10,531–18,986 ft)) and 2-D seismic data (1,450 km length and 9 seconds two-way time) [seismic and wells from TGS NOPEC]; stratigraphic and structural interpretations from this study, i.e. Mesozoic carbonate platform region and compressional and strike-slip structures.

Figure continued on facing page.

Results of the thermal modeling show that maturation of source rocks was a function of location in the basin, tectonic activity and age. Immature source rocks resulted from uplift during tectonic events or inadequate burial. The Messinian Salt hindered maturity of the younger source rocks. Vertical and lateral migration through carrier beds resulted in accumulation mostly in structural traps rather than stratigraphic traps. Uncertainties of the input parameters in the model were evaluated using a classic

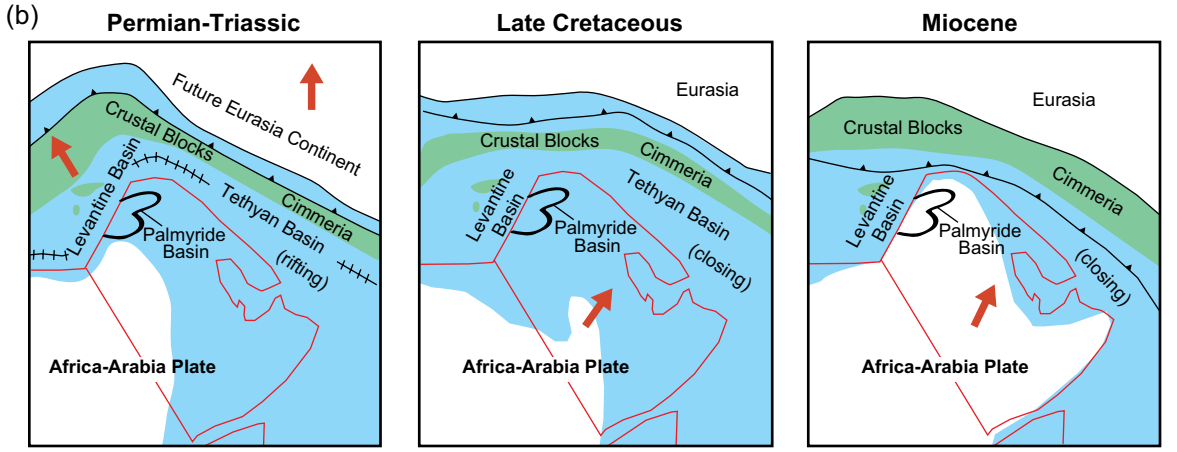

Figure 1 *(continued)*: (b) Paleogeographic reconstruction showing opening and closing of the Neo-Tethyan Sea and the relative position of the Levantine Basin with respect to the African-Arabian Plate and Neo-Tethyan Margin (blue indicates estimated area underwater along the southern margin).

approach of multiple-scenario simulation runs compared to a base model and risk analysis (Monte Carlo simulation) within PetroRisk. The classic approach used and varied input parameters that included heat flow, TOC percent, and source rock thickness, and suggests that with all models hydrocarbons have been generated and trapped though the volume produced varies from model to model. We concluded that the most critical parameters responsible for the volume of hydrocarbons potentially preserved in reservoirs are heat flow, TOC percent, thickness of source rock, and lithologic properties.

GEOLOGIC SETTING

The tectono-stratigraphic history of the Levantine Basin is largely a function of its position along the northern African and Arabian plates and southern Neo-Tethyan margin (Figure 1b). The Levantine Basin followed the tectonic progression of rift-extension, passive margin and compression associated with the break-up of Gondwana and collision of the African and Arabian plates and Eurasian Plate beginning in the Late Cretaceous (Figure 1b).

Rift-extension began in the Late Permian – Early Triassic when crustal blocks were detached from the African-Arabian plate margin (Figure 1b). While most blocks accreted onto the Eurasian Plate, two remained in the Eastern Mediterranean (Eratosthenes Seamount and Cyprus) (Figure 1) (Garfunkel, 1998; Robertson, 1998). The rift-extension resulted in a thinned continental crust; crustal thickness ranges from 10–20 km (offshore) to 35 km (onshore) (Netzeband et al., 2006). The rift-extension in the Levantine Basin was generally coincident with the formation of an adjacent basin, the Palmyride Basin, which is a failed rift basin to the east (Figure 1) (Sawaf et al., 2001; Mouty, 2000; Nader and Swennen, 2004). The rift and post-rift passive margin thermal subsidence associated with the Levantine Basin created an estimated 15 km of accommodation. Passive margin conditions dominated through much of the Jurassic (Walley, 1997, 2001). Compressional and strike-slip tectonics coincided with the collision of the African and Arabian plates and Eurasian Plate beginning in the Late Cretaceous (Figure 1b). Tectonic activity occurred in phases and resulted in several regional structures (Figures 1a and 2), including the NE- and NNE-trending folds (referred to as Syrian Arc folds), the structures of Lebanon (Mount Lebanon and Anti-Lebanon anticlines, Bekaa valley syncline), Levantine Hingeline (Western Lebanon Flexure), and the Dead Sea Transform Fault (Figure 1a; Robertson and Dixon, 1984; Walley 1998; Beydoun, 1999; Mart et al., 2005; Gardosh and Druckman, 2006; Schattner et al., 2006).

Since the Levantine Basin was part of the larger Neo-Tethyan Basin for much of its history, deposition was influenced by the Neo-Tethyan Ocean, which was an equatorial sea exposed to greenhouse conditions throughout most of the Mesozoic and Cenozoic. Depositional environments in the Levantine Basin and surrounding region ranged from continental to deep marine and resulted in a stratal package up

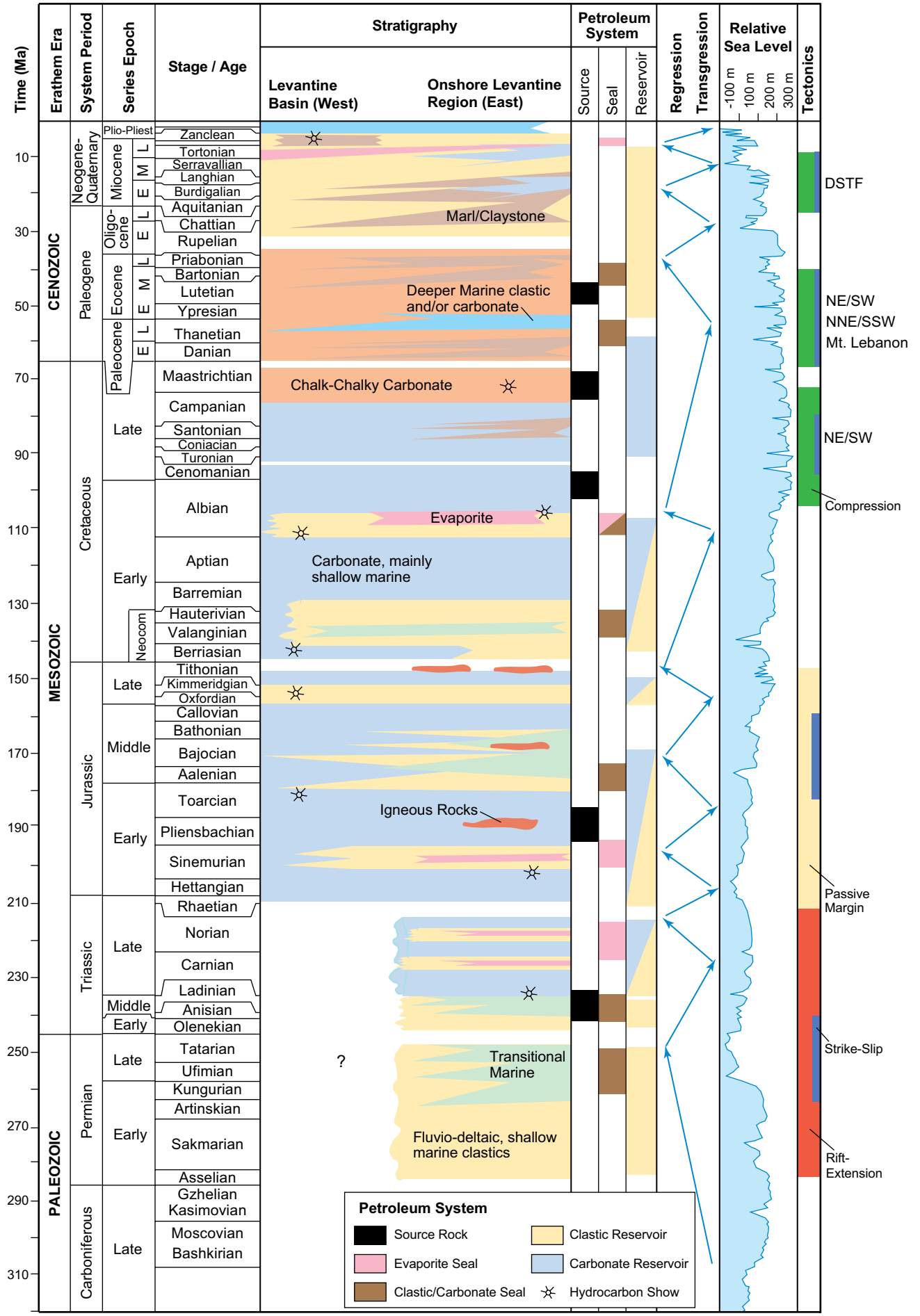

Figure 2: *See facing page for figure caption.*

to ca. 15 km thick consisting mostly of Mesozoic and Cenozoic carbonate-siliciclastic-evaporitic facies (Renouard, 1955; Hsu et al., 1977; May, 1991; Beydoun, 1993; Beydoun and Habib, 1995; Walley, 1997, 2001; Toland, 2000; Abdel-Rahman and Nader, 2002; Nader and Swennen, 2004; Flexer et al., 2005, Hirsch, 2005; Ben-Avraham et al., 2002; Bertoni and Cartwright, 2006; Gardosh and Druckman, 2006; Hubscher et al., 2007; Roberts and Peace, 2007). The Levantine Basin was thought to be a deep-water basin for most of its history (Stampfli et al., 2001). However, interpretations from this study suggest that much of the southern part of the basin was part of the primarily shallow-marine setting that dominated the region during the Mesozoic.

DATABASE AND METHODS

Database

The tectono-stratigraphic model for the basin was developed using 2-D seismic and well data provided by TGS NOPEC and regional analogs. The 2-D seismic data were acquired in 2001 and 2002 and cover 1,450 km with a depth coverage 9 seconds (two-way time) and more (estimated depth equivalent of 14–15 km) (Figure 1a). The seismic data were previously migrated and processed. Frequency for the seismic data ranges from 24–69 Hz, which equates to an approximate range of vertical resolution of 40–200 m (131–656 ft). The 4 wells for this project ranged in depth from 3,210–5,787 m (10,531–18,986 ft) and penetrated to Lower Jurassic rocks. Well data included chronostratigraphy, lithologic description, hydrocarbon show information, bottom-hole temperature, and numerous logs (spontaneous potential, resistivity, density, sonic, gamma-ray, neutron porosity, photoelectric, caliper, and tension).

Methods

Tectono-stratigraphic Model Development

The tectono-stratigraphic model describes the tectonics and deposition that occurred in the basin from Permian to recent. Tectonics and stratigraphy in the Levantine Basin were mapped as follows:

(1) the wells were tied to the seismic data using velocity, resistivity, density, and formation top data using SMT Kingdom Software.
(2) A chronostratigraphic framework was developed for the basin fill. The stratal package was divided into nine chronostratigraphic units (Figure 3); the chronostratigraphic surfaces were extended basinward from the wells by tracing reflections.
(3) Reflection terminations, off-set reflections, folded reflections, and seismic character changes were identified.
(4) Type and timing of tectonic settings were established by delineating structures in the basin (for example, folds, flower structures).
(5) The type and timing of depositional packages were delineated using well data, depositional models, sequence stratigraphic concepts and geomorphic interpretation (Mitchum et al., 1977; Vail et al., 1977; Read, 1985; Kendall et al., 1991; Emery and Myers, 1996; Posamentier and Allen, 1999; Pomar, 2001; Eberli et al., 2004; Schlager, 2005; Lukasik and Simo, 2008).
(6) Depositional packages were assigned facies. The facies were designated as source, seal or reservoir rocks based on well and regional data.
(7) Selected lines were converted from time sections to depth sections to be used in the 2-D petroleum system modeling.

Figure 2 (*facing page*): Tectono-stratigraphic history of the Levantine Basin based on well and seismic interpretations and regional analogs, including petroleum system elements and hydrocarbon shows. Tectonic settings are color coded and indicate timing of formation of regional structures: fold trends of NE/SW and NNE/SSW orientation; Mount Lebanon anticline; DSTF-Dead Sea Transform Fault. The relative sea level illustration is from Waite and Gilcrease (2002). Onshore data are simplified from a combination of sources: Renouard (1955), May (1991), Beydoun (1993), Beydoun and Habib (1995), Walley (1997, 2001), Toland (2000), Abdel-Rahman and Nader (2002), Nader and Swennen (2004), Flexer et al. (2005), Hirsch (2005); Gardosh et al. (2008); and Weissbrod (2005).

2-D Basin and Petroleum Systems Modeling

The 2-D basin and petroleum system model describes the burial and thermal history and provides insight into the timing of petroleum generation, migration and accumulation. The 2-D basin model parameters were constrained using the tectono-stratigraphic model, which is outlined in the next section. Values for each parameter were defined based on the tectono-stratigraphic interpretations, well data, regional analogs and the literature (Allen and Allen, 2005; Hantschel and Kauerauf, 2009).

Several input parameters were considered for the model some of which are described in a later section including age, facies, petroleum system elements, paleogeometry, heat flow, and calibration. Once the parameter values were established, the model was built within the PetroMod2D workflow using the depth converted seismic sections and wells. PetroMod2D provides the ability to build, simulate, view, and risk the model. Grid spacing of the model was established to give 300 m (984 ft) and 400 m (1,312 ft) per finite element cell for lateral and vertical resolution, respectively.

Sensitivity analyses were performed using the Monte Carlo simulation within PetroMod2D by selecting key parameters and giving them ranges of values consistent with the uncertainty in each measurement. Additional sensitivity analyses were achieved by creating several different models, varying selected input parameters, and comparing the results.

TECTONO-STRATIGRAPHIC MODEL

The spatial and temporal distribution of tectonics in the basin was separated into its various phases: rift-extension, passive margin, strike-slip, and compression (Figure 2). Rift-extension initiation was estimated at Permian – Triassic. Extension resulted in thinning of the continental crust to an estimated 10–20 km (Netzeband et al., 2006). Rifting was followed by a Jurassic passive margin thermal subsidence phase. Strike-slip and compressional tectonics were most active during the Late Cretaceous, Paleocene and Miocene (Figure 2). Strike-slip and compressional tectonics are evidenced by numerous structures such as flower structures and folds, respectively (Figure 3). Flower and fold structures are concentrated at the eastern margin of the basin and they are laterally extensive in a north-south direction; minor compressional folds also exist basinward (Figures 1 and 3). Strike-slip and compressional structures are also prevalent onshore: the Dead Sea Transform Fault (DSTF), which was initiated in the Miocene, is responsible for 107+ km of sinistral offset (Beydoun, 1999) and there are numerous NNE- and NE-trending folds, including the Mount Lebanon and Anti-Lebanon anticlines, which reach elevations of 3,088 m (10,131 ft) and 2,813 m (9,229 ft), respectively (Figure 1).

Strata in the Levantine Basin is estimated to be ca. 15 km (49,212 ft) thick and are composed of mixed carbonate-siliciclastic-evaporite facies that resulted from a full range of depositional environments from continental to deep marine, although shallow marine carbonate environments dominated (Figure 2). The stratal package probably overlies Proterozoic basement similar to that onshore (Flexer et al., 2005; Hirsch, 2005).

Well data in the basin only goes back to the Lower Jurassic. However, earlier history can be extrapolated from onshore data. If there are Paleozoic strata in the basin, they are likely a thin package of mostly siliciclastics (thickness possibly < 1 km (3,280 ft)). Onshore Paleozoic strata consist of siliciclastics that were deposited in mostly fluvio-deltaic environments (Weissbrod, 2005). The Permian – Triassic strata in the basin are probably a mixture of carbonates, siliciclastics, and evaporites deposited in alternating carbonate platform/interplatform and fluvio-deltaic environments similar to nearby onshore correlatives (Flexer et al., 2005) (Figure 2) as well as distal potential correlatives (Murris, 1980; Sharland et al., 2001; Sadooni and Alsharhan, 2004). Onshore, deposition was interrupted by subaerial exposure that resulted in karstification of some carbonates and paleosol development (Gardosh and Druckman, 2006). Evaporites are also a significant part of the Permian – Triassic section onshore and they appear to extend into the basin. The potential evaporite deposit that may be in the basin would be a part of the regionally extensive Upper Triassic Kurra Chine Formation, which includes the Kurra Chine Salt (Figure 1) (Nader and Swennen, 2004). Onshore this is a significant deposit that is important to many petroleum systems in the region (Sawaf et al., 2001; Nader and Swennen, 2004; Sadooni and Alsharhan, 2004). The existence of the Kurra Chine Salt in the Levantine

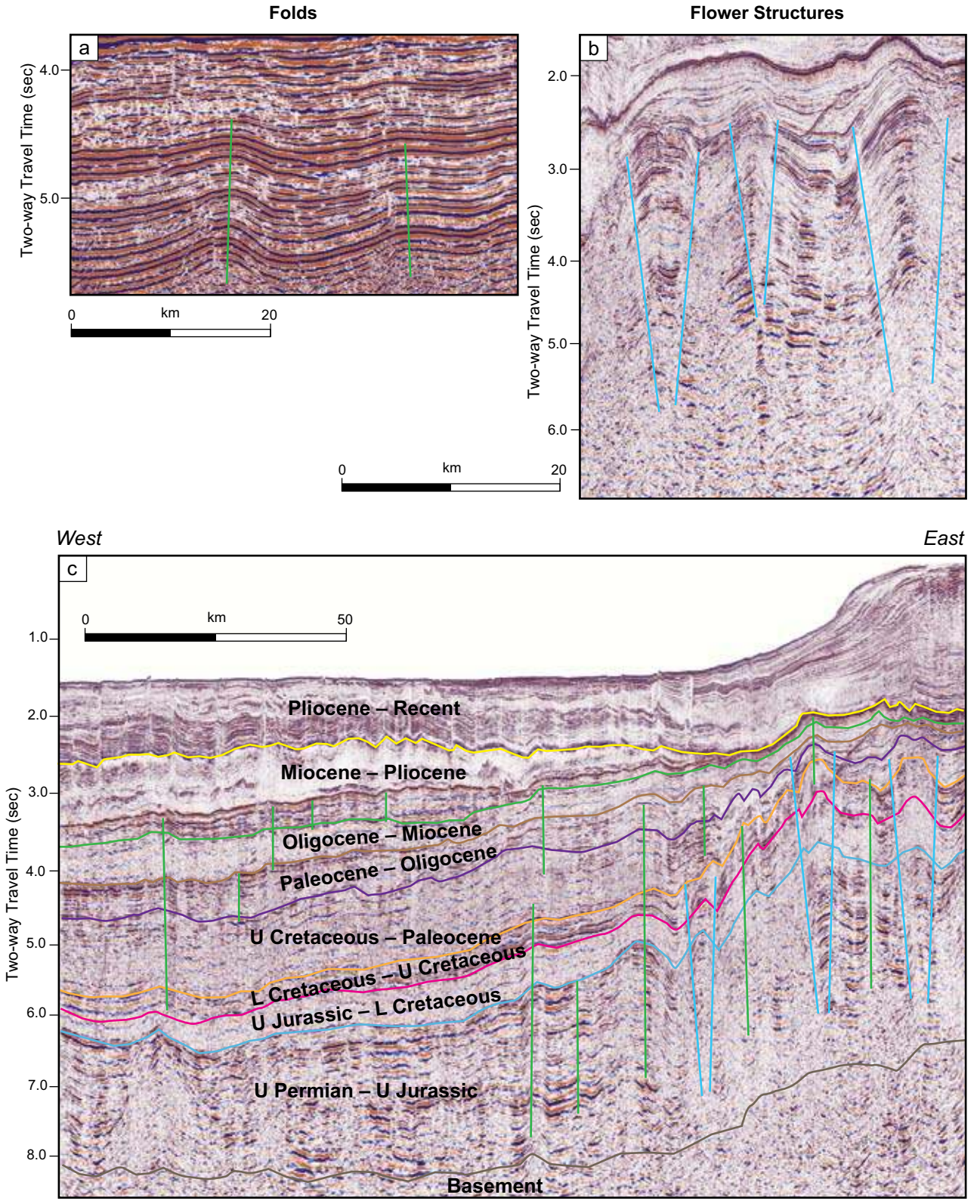

Figure 3: Delineation of chronostratigraphic packages and examples of structural features in the Levantine Basin related to the compressional (green) and strike-slip (blue) faults; these features were used to bracket the timing and distribution of the compressional and strike-slip tectonics in the basin. (a) Folds - compressional; (b) flower structures - strike-slip, and (c) distribution of folds and flower structures in the basin; although structures exist spatially throughout the basin, the major structural deformation occurs in the eastern part (see Figure 1 spatial distribution of interpreted compressional and strike-slip structures)(seismic data compliments of TGS NOPEC).

Basin has been proposed (Beydoun and Habib, 1995; Nader and Swennen, 2004) and interpretations from this study indicate that a possible deep salt (a Kurra Chine equivalent) may be responsible for salt diapirs (Figure 4).

Jurassic strata are a mixture of carbonate with some siliciclastics. Seismic and well interpretations suggest that the carbonate was deposited in a carbonate platform (shallow water) and interplatform (deeper water) environment that probably alternated with fluvio-deltaic periods and/or by-pass deposits (Figure 5). There are numerous carbonate platforms throughout the southern part of the basin in the region delineated in Figure 1. The spatial distribution and the variability in size of the carbonate platforms and interplatform basins is analogous to a 3-D representation of the Miocene carbonate platforms in Sarawak, Borneo (Figure 5c and d) (Vahrenkamp et al., 2004). Seismic character of the platform core is chaotic-transparent (Figure 5a); talus-turbidite-interplatform deposits onlap the main body of the platform (Figure 5b). The diameters of the platforms in the Levantine Basin

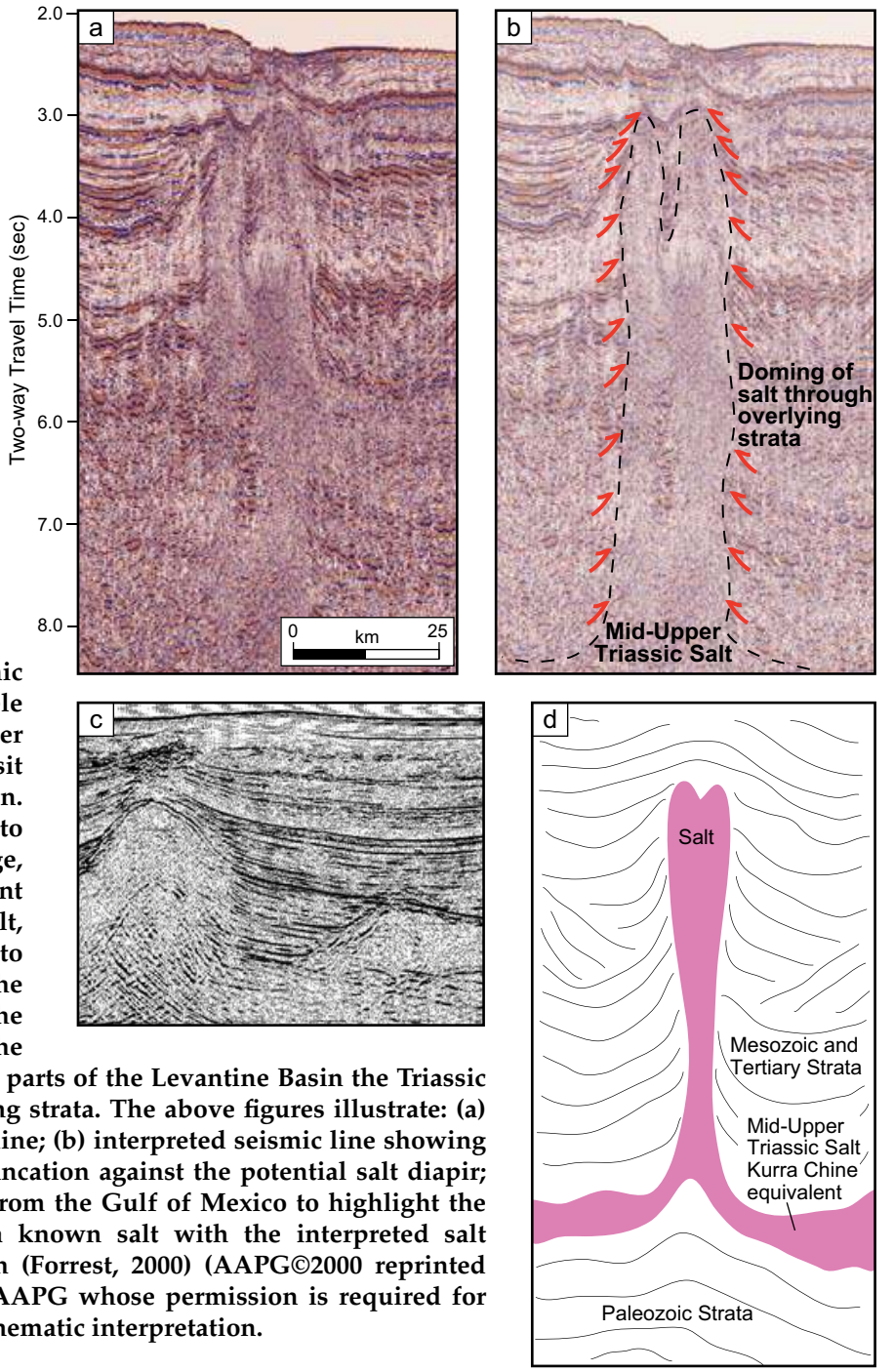

Figure 4: Seismic evidence of possible salt diapir from Lower Mesozoic salt deposit in the Levantine Basin. The salt is likely Mid to Upper Triassic in age, possibly the equivalent to the Kurra Chine salt, which is thought to have extended into the Levantine Basin from the Palmyride Basin to the northeast (Figure 1). In parts of the Levantine Basin the Triassic salt penetrates overlying strata. The above figures illustrate: (a) uninterpreted seismic line; (b) interpreted seismic line showing stratal terminations/truncation against the potential salt diapir; (c) known salt diapir from the Gulf of Mexico to highlight the similarities between a known salt with the interpreted salt of the Levantine Basin (Forrest, 2000) (AAPG©2000 reprinted by permission of the AAPG whose permission is required for further use); and (d) schematic interpretation.

range from 10–75 km and the thicknesses range from 2–6 km (ca. 6,500–19,685 ft). These carbonate platforms are similar to those of the Apulia Platform, which also evolved along the Neo-Tethys Ocean during the Jurassic and Early Cretaceous and have comparable thicknesses (up to 6 km thick) (19,685 ft) (Bosellini, 2004).

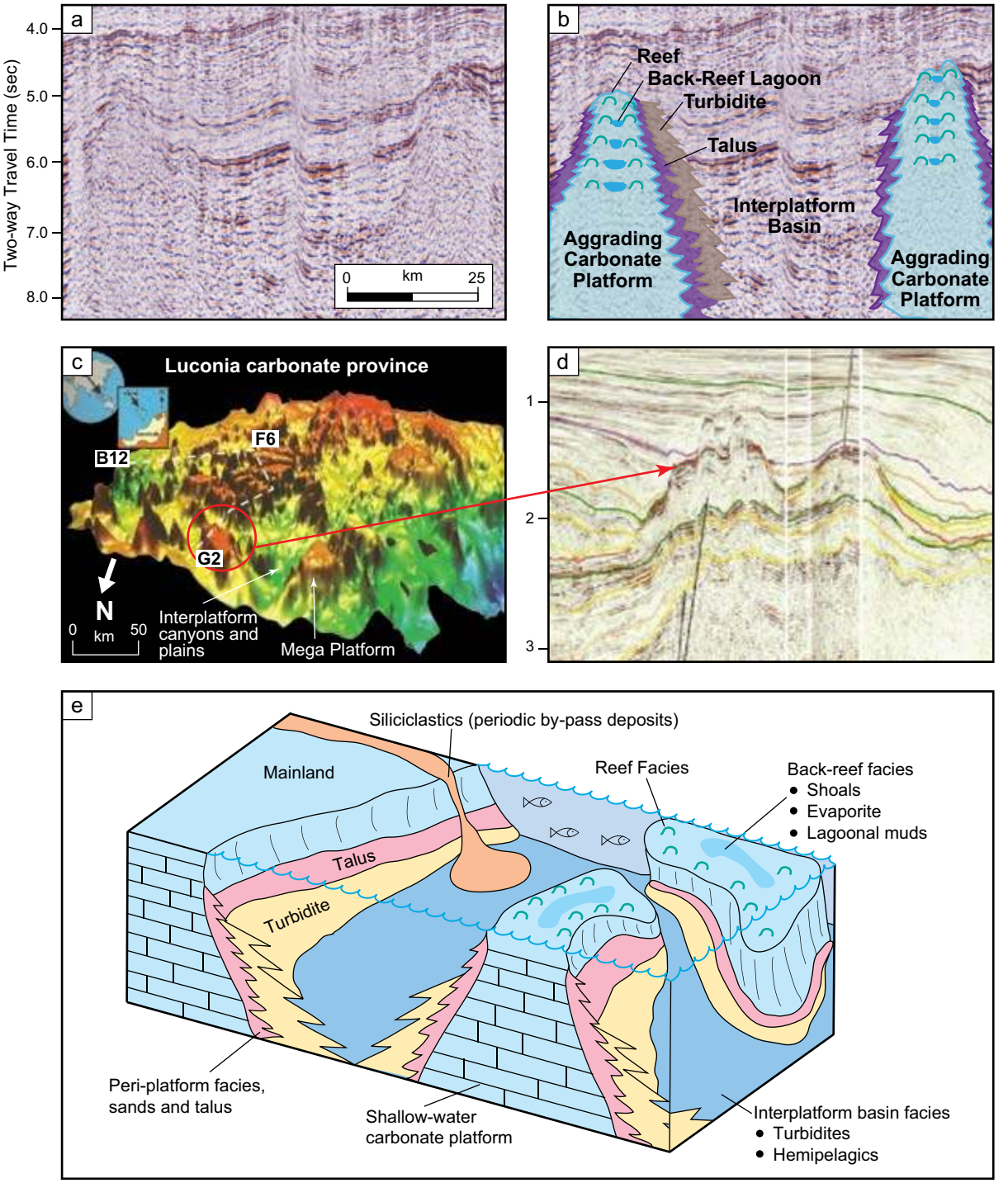

Figure 5: Carbonate Platform and Interplatform Basins of the Mesozoic section of the Levantine Basin: (a and b) Uninterpreted and interpreted lines from the Levantine Basin; (c and d) 3-D image and seismic image of the Miocene Carbonate Platform Luconia Province, offshore Sarawak, Borneo (Vahrenkamp et. al., 2004) (AAPG©2004 reprinted by permission of the AAPG whose permission is required for further use); and (e) Schematic of the depositional environment that dominated the early part of the Mesozoic in the Levantine Basin; a mixed carbonate and siliciclastic system. (Modified from Read, 1985).

The Levantine platforms exhibit mostly aggradational-retrogradational growth patterns. Carbonate deposition was also prevalent on present-day onshore during the Jurassic. To the east of the basin carbonate thickness ranges from ca. 1.5 km (4,920 ft) (Gardosh et al., 2008) to possibly more than 2 km (6,560 ft) (Walley, 1997).

From Late Jurassic – Early Cretaceous there is an increase in siliciclastic strata deposited in shallow-marine to fluvio-deltaic environments; however, carbonates also persisted. Block faulting and associated volcanism at this time likely affected sedimentation (Walley, 1997). Rising sea level led to deep-water conditions that persisted from the Late Cretaceous through the Eocene. Deposition during this time was dominantly chalk and chalky carbonate deposits on present day onshore (Walley, 1997) and in the basin.

A major regression began in the Oligocene and continued into the Miocene. The regression led to several events: (1) erosion and redeposition of previously deposited strata, (2) canyon formation on the shelf (Druckman et al., 1995; Buchbinder and Zilberman, 1997), and (3) deposition of the Messinian Salt. Seismic interpretations of reflection terminations (toplap, onlap, downlap, truncation) illustrate the erosion and subsequent deposition of sediments (Figure 6).

Siliciclastic deposition dominated, however, there was possible remobilization of older chalky strata during erosional events. Overlying the dominantly siliciclastic package of the Oligocene and Miocene is the Messinian Salt, one of the largest evaporite deposits in the world, which exceeds 2 km (6,560 ft) in thickness in the deeper part of the basin and pinches out near the modern continental shelf (Figure 6; Bertoni and Cartwright, 2006). Pliocene to Recent siliciclastic strata were deposited in a mostly deeper-water setting. At present most of the basin is in 1,000–2,000 m (3,280–6,561 ft) of water (Figure 1).

MODEL INPUT

Ages-Deposition

The stratal package was divided into nine chronostratigraphic units (Table 1 and Figure 3), which were further split into multiple layers to improve facies assignment and delineation. Chronostratigraphic units were chosen based on well information for those stratal units Early Jurassic and younger. Although there are documented unconformities onshore (Figure 2) estimates for erosional thickness are not available and it was assumed the thickness lost would not significantly affect the burial history of the basin.

Lithofacies and Petroleum System Elements

Lithofacies for the model were chosen based on their occurrence and expected occurrence from the stratigraphic and depositional interpretations of wells and seismic. Well data documents a wide range of lithofacies in the basin. However, only a select few were chosen for the stratigraphic model (Table 2). Many of the facies chosen to represent the basin stratigraphy are in the PetroMod library; however, lithofacies combinations were also created that are representative of depositional environments. The lithofacies and combinations of lithofacies were assigned to the seismic section according to stratigraphic interpretations and depositional environment. Material properties associated with the lithofacies are summarized in Table 2.

Petroleum system elements were defined for the stratal package including, candidate source, seal, reservoir, and overburden rocks. Source rocks in the system are postulated to be carbonate muds and shales. Five source rock periods were assigned (Table 3); these source rock periods (Triassic, Lower Jurassic, Lower and Upper Cretaceous, and Eocene) are consistent with other regional source rock deposition (May, 1991). The source rock properties, including total organic carbon (TOC), hydrogen index (HI), and kinetics were chosen based on information from the wells and interpretations of the seismic data set, along with regional analogs (Table 3). There was no direct evidence for these parameters from the Levantine Basin. Since there were no measurements of TOC available from the basin, the TOC values assigned to potential source rock intervals were intentionally kept low, between

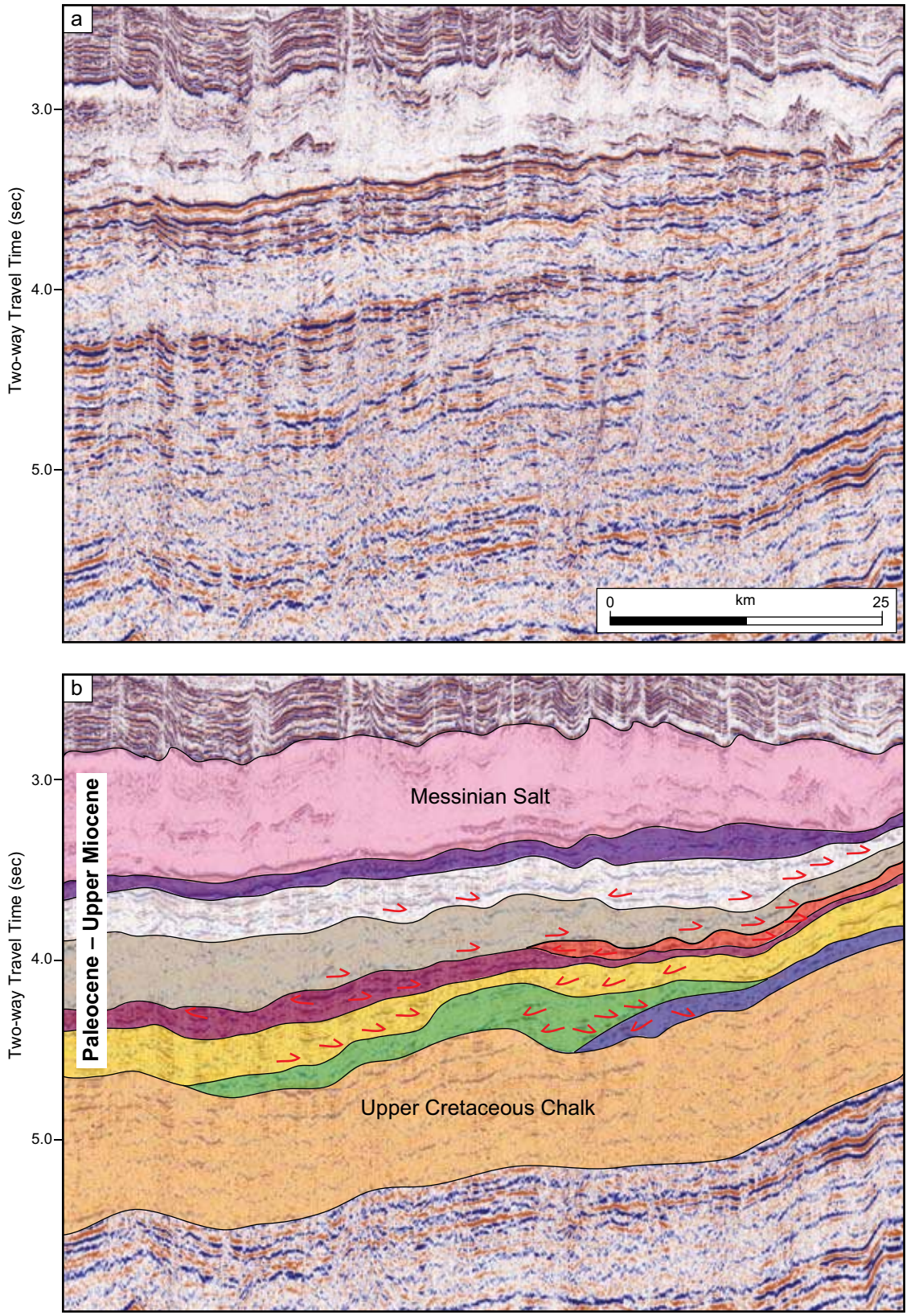

Figure 6: Pre-Messinian strata deposited between the Messinian Salt and Upper Cretaceous chalk is a Paleocene – Miocene stratal package dominantly siliciclastics. A series of erosional events and deep-water deposition occurred resulting in stacked turbidite deposits.

Table 1
Age definitions for the seismic depth sections (software for modeling is PetroMod2D from Schlumberger)

5-0 Ma	Pliocene - Recent
11-5 Ma	Miocene - Pliocene
33-11 Ma	Oligocene - Miocene
65 - 33 Ma	Paleocene - Oligocene
99 - 65 Ma	Upper Cretaceous - Paleocene
144- 99 Ma	Lower Cretaceous - Upper Cretaceous
159- 144 Ma	Upper Jurassic - Lower Cretaceous
206 - 159 Ma	Upper Triassic - Upper Jurassic
256 - 206 Ma	Upper Permian - Upper Triassic
290 - 256 Ma	Basement

Table 3
Source rock periods and associated properties used in the model. Ages of source rocks are 235, 190, 100, 75, and 45 Ma

Source Rock	Age, MA	Lithology	TOC, wt %
Eocene	45	Marl	1
Upper Cretaceous	75	Chalky LS	2
Lower Cretaceous	100	Mixed SH 10%	3
Lower Jurassic	190	Limestone	2
Lower Jurassic	190	Mixed Shale 10%	3
Triassic	235	Shale	3

* Hydrogen Index (mg HC/g TOC) = 500 for all
* Kinetics = Pepper and Corvi (1995) Type IIB for all
* Lower Jurassic has two types of source rock to reflect different depositional environments
* Mixed Shale 10% is a combination of lithologies, the shale with TOC 3% component is 10% of the lithologic unit

Table 2
Lithologies and associated material properties in the 2-D Model; lithologies and data from the PetroMod2D library

Name	Lithology (%)	Density	Surface Porosity - Max Compaction Porosity	Thermal Conductivity	Permeability	Mass Heat Capacity	Radiogenic Heat Production	Uranium	Thorium	Potassium
		kg/m^3	(%)	W/m/K 20°C /100°C	log mD	kcal/kg/K 20°C/100°C	micro W/m^3	ppm	ppm	ppm
Marl	Marl (100)	2,700	50 - 1	2.0 / 1.96	(-0.78) to (-5.05)	0.203 / 0.234	0.71 - 1.18	2.5	5	2
Chalky LS	Chalky LS (100)	2,680	65 - 1	3.2 / 2.84	(-0.54) to (-6.75)	0.206 / 0.238	0.36 - 0.60	1.9	1.4	0.25
Limestone-source	LS-2% TOC (100)	2,710	51 - 1	2.63 / 2.42	(1.0) to (-1.99)	0.201 / 0.232	0.47 - 0.79	2.5	1.7	0.27
Mix-source	LS (25); LS 1-2% TOC (30); SH (25); SS (15); Gypsum (5)	2,672	48 - 1	2.33 / 2.24	(-0.54) to (-4.41)	0.208 / 0.240	0.61 - 1.01	2.45	4.29	1.04
Shale-source	SH 3% TOC (100)	2,610	70 - 1	1.45 / 1.55	(-1.0) to (-8.52)	0.21 / 0.243	1.3 - 2.3	5	12	2.8
Limestone-no source	LS micrite (100)	2,740	51 - 1	3 / 2.69	(-1.52) to (-2.02)	0.2 / 0.231	0.21 - 0.35	1	1	0.2
Mix-no source	SH organic lean (30); LS micrite (30); SS (30); Gypsum (10)	2,680	49 - 1	2.56 / 2.40	(-0.25) to (-5.36)	0.209 / 0.242	0.55 - 0.92	1.81	4.97	1.29
Shale-no source	SH organic lean, sandy (100)	2,700	65 - 1	1.84 / 1.84	(-1.0) to (-8.42)	0.206 / 0.238	1.03 - 1.71	2.8	11	2.5
Sandstone	SS (100)	2,720	41 - 1	3.95 / 3.38	(-4.33) to (-1.8)	0.204 / 0.236	0.42 - 0.70	1.3	3.5	1.3
Limestone	LS (100)	2,740	35 - 1	3.0 / 2.69	(-3.0) to (-2.44)	0.200 / 0.231	0.21 - 0.35	1	1	0.2
Anhydrite	Anhydrite (100)	2,970	1	6.3 / 5.11	0	0.179 / 0.207	0.06 - 0.09	0.1	0.3	0.4
Salt	Salt (100)	2,740	1	6.5 / 5.25	0	0.206 / 0.238	0.01 - 0.02	0.02	0.01	0.1
Granite	Granite (100)	2,700	5	3.0 / 2.65	-16	0.188 / 0.233	0	0	0	0
Granite Hot	Granite (100)	2,700	5	3.0 / 2.65	-16	0.188 / 0.233	1.67 - 79	4	20	4

*Radiogenic heat production ranges with porosity and ppm of U, Th, K

1–3%, in order to keep the model conservative. Regional TOC values associated with source rocks that were deposited as part of the Neo-Tethyan Ocean system have contained > 10% TOC (Beydoun, 1993; Fox and Ahlbrandt, 2002; Pollastro, 2003;).

Hydrogen Index (HI) values of 500 mg/TOC were chosen to match the average value of the known Jurassic source rocks (Pollastro, 2003). Hydrogen indices are generally associated with the type of kerogen and indicate whether a source rock is oil-prone or gas-prone. Type II kerogen is characteristic of shallow-marine basins and is most common in petroleum systems of the Arabian Peninsula (Beydoun, 1993; Pollastro, 2003). The kinetics (Pepper and Corvi, 1995, Type IIB), were chosen based on the expected Type II kerogen for the basin.

Reservoir potential exists from the carbonate and siliciclastic strata. Reservoir rocks in the system are likely to be primarily sandstone, limestone, dolomite, or chalk. Candidate seals are carbonate, siliciclastic and evaporitic, namely, limestone, dolomite, marl, shale, anhydrite, and salt.

Paleogeometries and Structure

Paleogeometries and structure were accounted for by the model. Initial basin topography was assumed to be relatively flat. Structures in the basin were corrected through time so that the pretectonic topographic expression of the basin was represen ted in the model.

Thermal Parameters

The thermal boundary conditions for this model are basal heat flow and surface temperature. The most important thermal parameter is basal heat flow. Basal heat flow is a function of the thickness of the crust, which is estimated at 10–20 km, and tectonic activity in the basin. Values for heat flow were chosen to reflect the changing tectonic settings (Figure 7; Allen and Allen, 2005). Granitic crust was used as the base layer (Netzeband et al., 2006). There is no evidence to support crustal basement in the

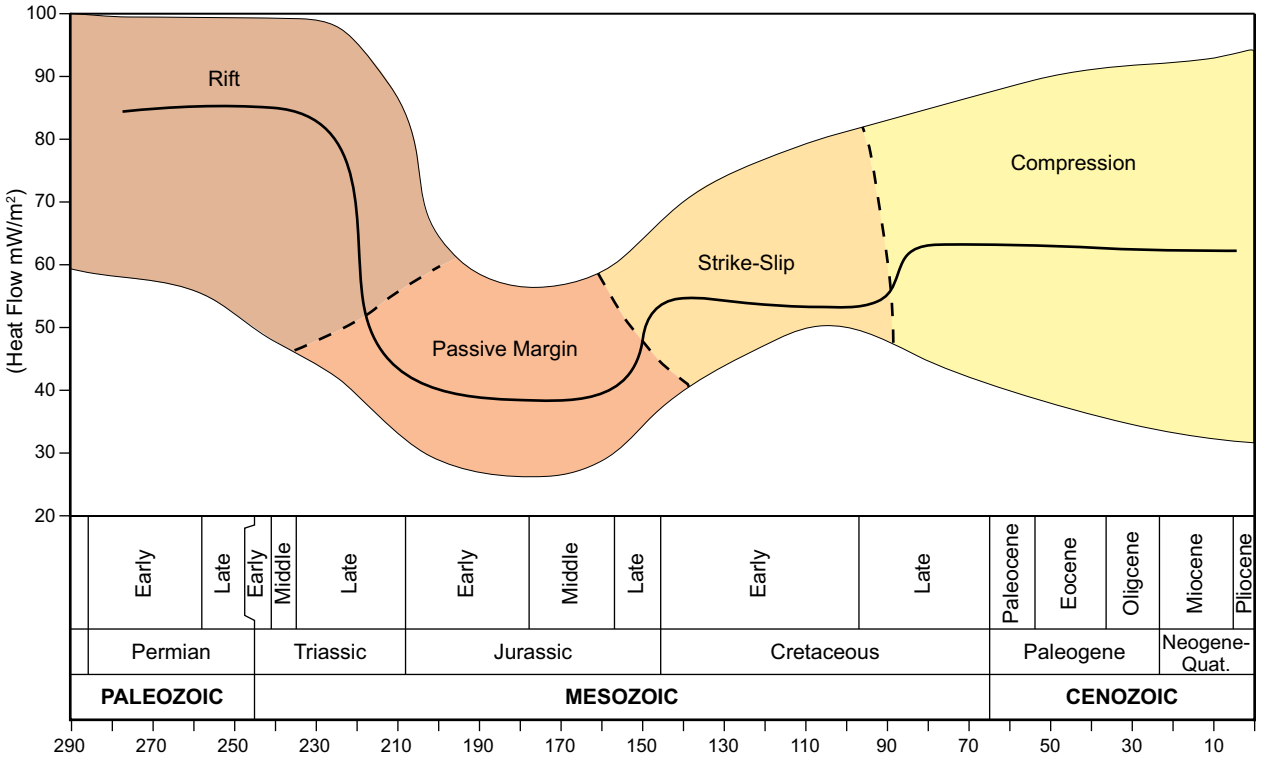

Figure 7: Basal heat-flow values assigned to the model over time. The values assigned are based on tectonic interpretations from the basin and they are within the range of heat-flow values estimated for various tectonic settings (Allen and Allen, 2005).

seismic sections. However, granitic crust is presumed to be the basement in the Levantine Basin so it was included in the model. The other boundary condition, surface temperature, paleolatitude through time, which for the basin was between 0–30° latitude for most of the time period of this model.

Other components that affect the heat budget are also accounted for by the model, such as the radiogenic heat from the granitic crust and mud-rich sedimentary rocks, and thermal conductivity. Radiogenic heat flow is a function of the amount of potassium (K), uranium (U), and thorium (Th) in the rocks (Table 2). Radiogenic heat from sedimentary rocks varies with the mud content. The more mud-rich rocks have higher radiogenic heat (Table 2). Thermal conductivity affects the heat budget through its affect on the rate of transmission of heat and it varies with lithology (Table 2). The Messinian Salt is the greatest heat conductor in this system.

Calibration of Heat flow

Calibration data are minimal for this basin. The primary calibration for the geothermal setting is bottom-hole temperature from the wells. Bottom-hole temperatures were corrected using a relationship developed by Harrison et al. (1983). The correction factor was added to the bottom-hole temperature to counteract the cooling effect of drill fluids on the temperature measurement. Paleotemperatures for the basin could not be calibrated as neither vitrinite reflectance nor apatite fission track data, which are two commonly used proxies for paleotemperatures, are available. Although measured calibration data are limited, the heat flow values assigned to the basin are reasonable because they are based on tectonic history interpretations and accepted heat flow values for a particular tectonic setting outlined in Allen and Allen (2005).

Hydrocarbon Generation, Expulsion and Migration

Thermal maturation of a source rock is a function of temperature, depth of burial, source rock properties (kinetics, HI, TOC) and time. Source rocks were tracked to determine timing of generation and transformation of kerogen. Expulsion into carrier beds and migration was modeled using four different models of fluid flow: Darcy, flow path, hybrid, and invasion percolation (Hantschel and Kauerauf, 2009). The Darcy flow method describes multicomponent three-phase flow and depends on relative permeability, viscosity and capillary pressure. The Darcy method has inherent disadvantages, such as long computation times, and may not be well suited for modeling migration (Hantschel and Kauerauf, 2009). Flowpath emphasizes the importance of lateral flow of petroleum in carrier beds along geometrically defined pathways. It is utilized to visualize lateral flow beneath a seal across entire drainage areas into an accumulation and it is especially suited for high permeability strata. The hybrid method is a combination of Darcy and flowpath and it facilitates analysis of flow in low-permeability regions (Darcy) and analysis of high-permeability areas, flow pathways, and accumulation sites (flowpath). The invasion percolation method assumes instantaneous movement of petroleum through buoyancy and capillary pressure. Invasion percolation is good for high and low permeability strata (Hantschel and Kauerauf, 2009). Although all of the migration methods were explored for this project, the results of this study are based on the invasion percolation method.

BASIN AND PETROLEUM SYSTEMS MODELS

Thermal and Burial History

Basin models provide insight into thermal and burial history. The basin model for this study suggests a temperature difference in the basin from west to east. Geothermal gradients in the basin that range from 1.3–2.0 to 2.5–2.8°C/100 meters on the west and east, respectively (Figure 8). Eastern temperatures are consistent with recorded geothermal measurements onshore (Greitzer and Levitte, 2005). Paleotemperatures for the basin were modeled using corrected bottom-hole temperatures from wells and calculated estimates based on the Sweeney and Burnham (1990) "Easy-Ro" kinetic reaction scheme since direct proxies for paleotemperature, such as apatite fission track or vitrinite reflectance measurements, are not available. The kinetics of Sweeney and Burnham are commonly used for basin modeling because they incorporate a chemical kinetic model that calculates vitrinite composition as

a function of temperature and time. Basin models such as this one provide predictions of porosity, permeability, and pressure based on the inputs and the tectono-stratigraphic model developed. The burial history of the basin shows a rapid increase in burial rate from the Late Cretaceous to present (Figure 9). Sedimentation rates vary from ca. 50–165 m (164–541 ft)/Ma with the exception of the Messinian Salt, which had a higher sedimentation rate. Sedimentation rates were determined for strata that were backstripped and decompacted within the model using porosity *versus* depth curves for different lithologies (Hantschel and Kauerauf, 2009).

Porosity and permeability of lithofacies change with burial. Depositional porosity ranged from 70–40%, but most strata below the Messinian Salt throughout the basin have porosities that decreased to 20% or less at depths exceeding 8,000 m (26,246 ft) where porosity may have decreased to less than 5% (Figure 10 and Table 2).

Pressures in the basin can be significant given the depth of burial and amount of compaction expected (Figure 10). Lithostatic pressure reaches a maximum of 350 MPa. Overpressure may be an issue in this basin (Figure 10). The pressure curves suggest that all strata below the Messinian Salt are overpressured and strata directly below the salt to a depth of 7.5 km (24,606 ft) may have abnormally high overpressure (> 50 MPa). Overpressure is caused from several mechanisms, the two most common mechanisms are probably rapid deposition of sediments and the resultant stress it causes on underlying strata and fluid expansion (Swarbrick et al., 2002). Fine-grained lithologies and low permeability strata, such as mudrocks, chalk, and salt, generally increase the magnitude of overpressure. Overpressure also results from fluid movement as well as other processes related directly to hydrocarbon generation and migration i.e. transformation of kerogen to oil/gas and buoyancy (Swarbrick et al., 2002; Hansom and Lee, 2005).

In our model the mechanism for overpressure is undercompaction caused by the impermeable Messinian Salt; the effect from hydrocarbon generation has also been taken into account, however, this effect will be magnitudes lower than that of the Messinian Salt. Though overpressure is often considered a negative, it can also have the positive effect of maintaining porosity and permeability (Hantschel and Kauerauf, 2009). Hence, the porosity and permeability of some of the sub-Messinian strata may be higher than represented (Figure 10), which would have implications for reservoir quality.

For the timescales covered in this project, the sedimentation rates and subsidence rates are considered approximately equal. Using that assumption, the sedimentation-subsidence rates were examined for a tectonic signature. Given the rift to passive margin tectonic setting from Permian – Jurassic a higher subsidence rate should be followed by a lower subsidence rate (Allen and Allen, 2005). Based on the subsidence rate (sedimentation rate) indicated by the model over that time period there is no clear signal indicating a rift-passive margin setting (Figure 9). This is assumed to be because the entire pre-Triassic strata is not visible on the seismic sections and therefore was not represented in the model. Subsidence is overall higher in the latter part of the history of the basin (Late Cretaceous to Recent).

Given the latter part of the basin's history was dominated by compression and strike slip resulting from the collision of plates and subduction to the north at the Cyprus Trench (Figure 1) and elsewhere, a foreland-basin signature might be expected. A foreland-basin signature is characterized by lower followed by higher subsidence rates (Allen and Allen, 2005). There is a higher subsidence rate for the Late Cretaceous – Eocene compared to the Early Cretaceous, indicating a possible foreland-basin signature (Figure 9).

Hydrocarbon Generation, Expulsion, Migration and Accumulation

Timing and the extent of generation of hydrocarbons (transformation) from the five source rocks was a function of location in the basin, tectonics, temperature, age and burial depth. The two oldest source rocks (Triassic-235 Ma and Lower Jurassic-190 Ma) are mature regardless of location within the basin (Figure 11). These source rocks were deposited well before the folding that occurred beginning in the Late Cretaceous, so maturation was uninterrupted. Transformation of the Triassic and Lower Jurassic source rocks into hydrocarbons occurred within 2–4 km (6,561–13,123 ft) depth and it took 90 and 75 My for the source rocks to be completely transformed, respectively (Figure 11).

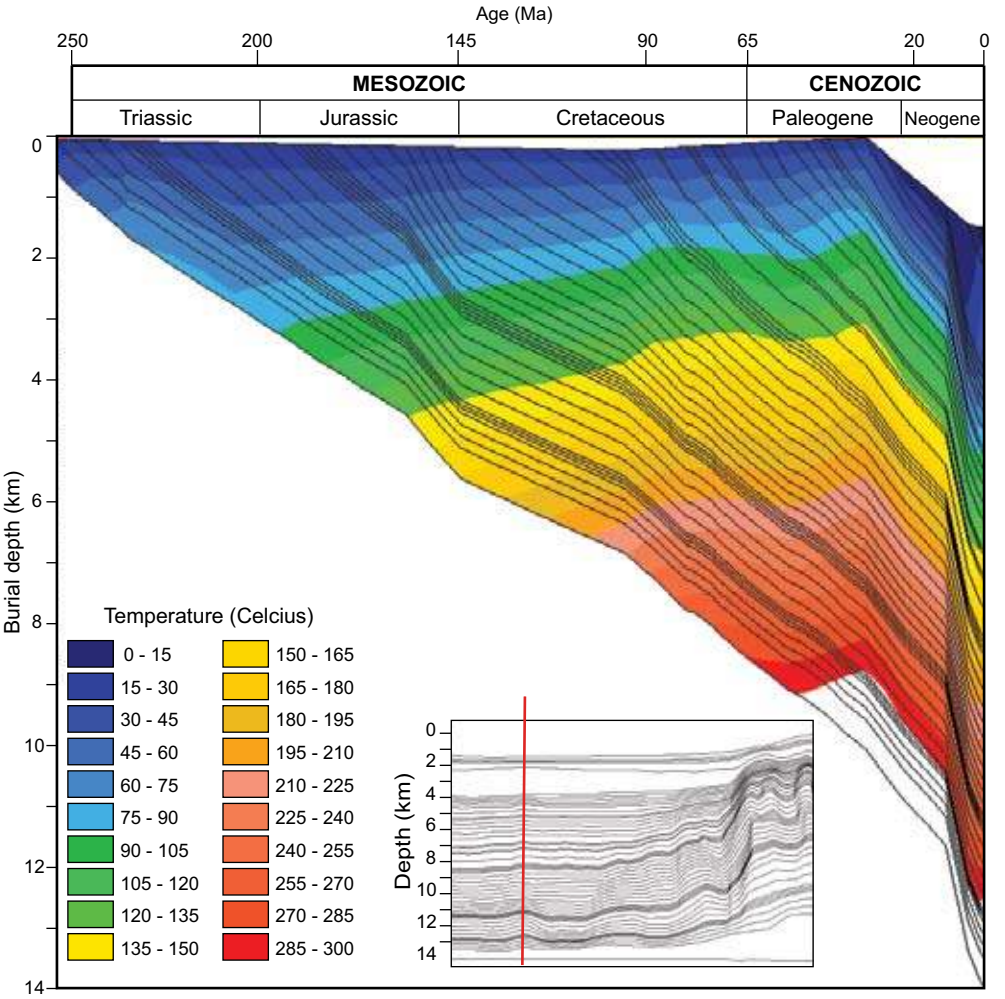

Figure 8: Temperature profile for the western part of the basin; the maximum temperature was 350°C. The 2-D Model suggests that geothermal gradients range between 1.3–2.0 to 2.5–2.8°C/100 m in the west and east, respectively. Inset indicates where measurements illustrated in figure were taken.

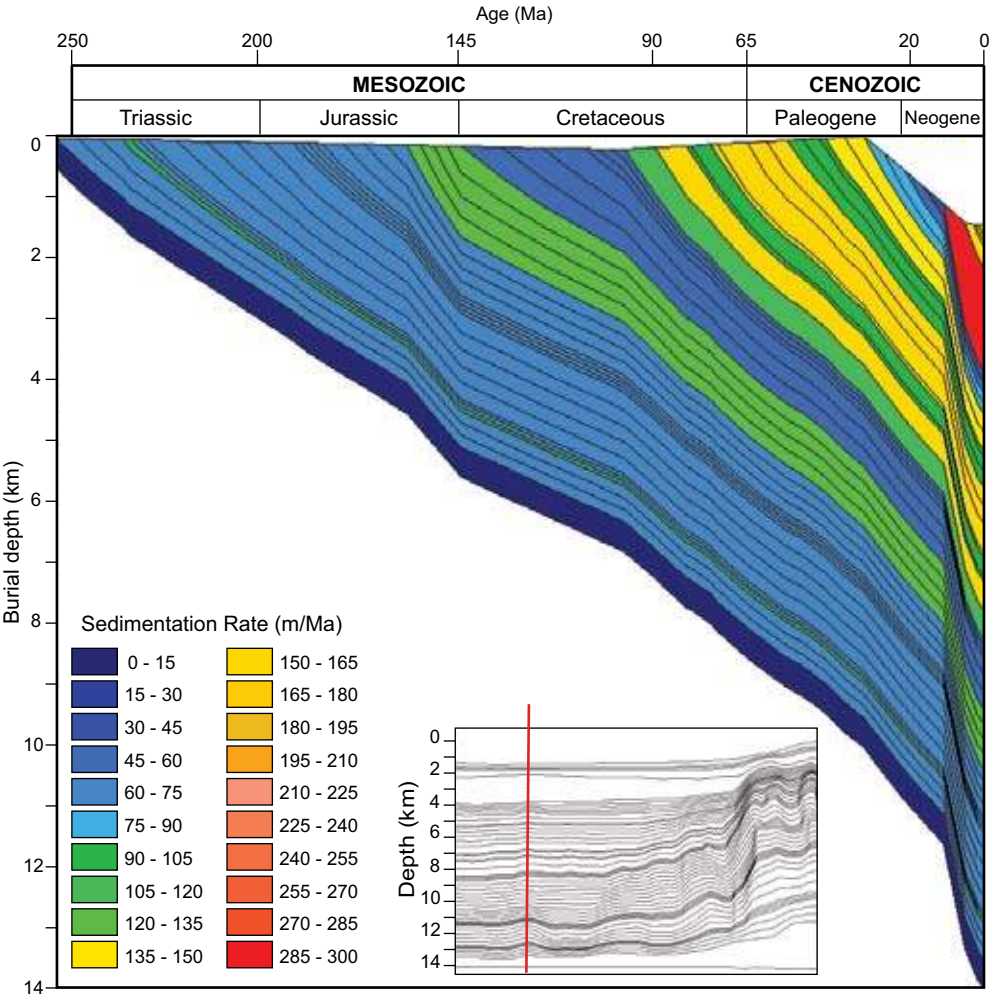

Figure 9: Burial history of the Levantine Basin. Inset indicates where measurements illustrated in figure were taken.

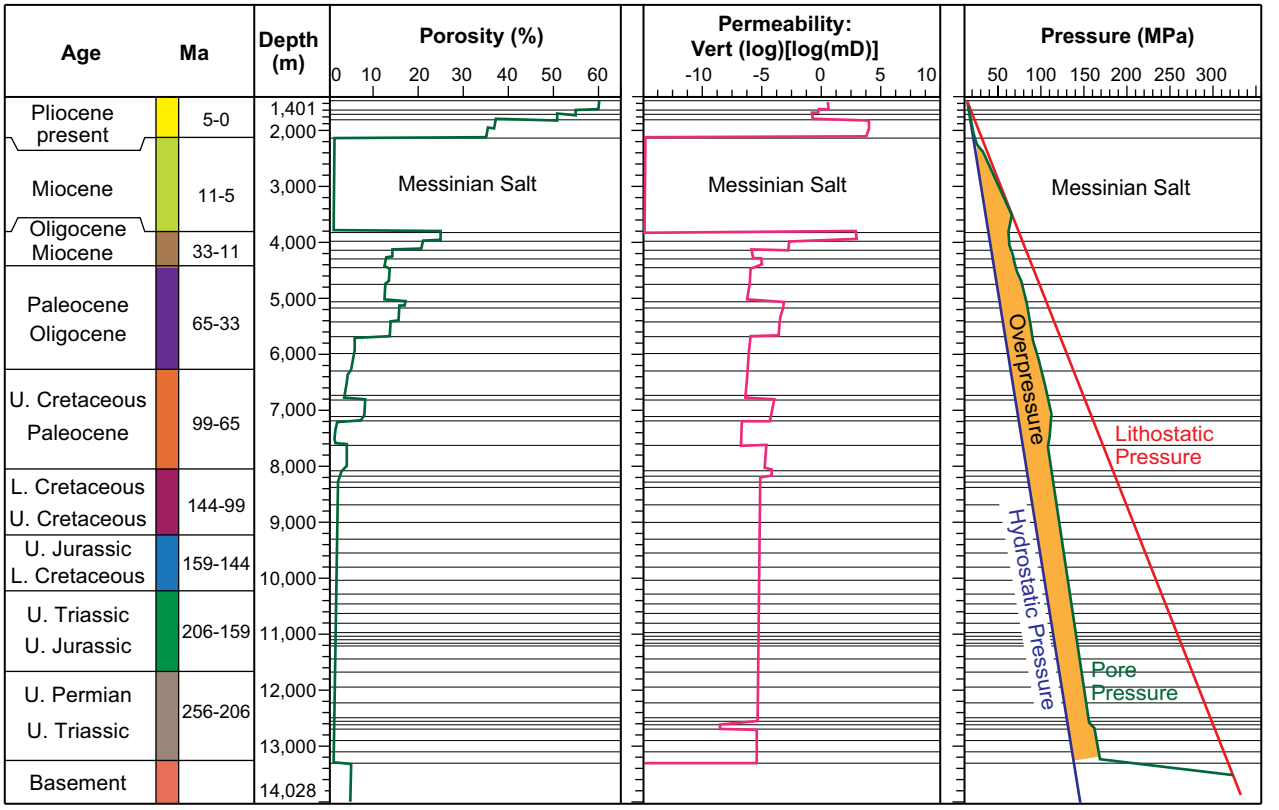

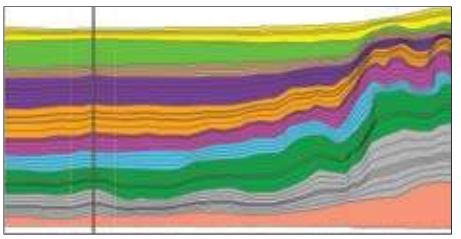

Figure 10: Porosity, permeability and pressure profiles with depth in the western part of the basin. Lithostatic pressure, pore pressure, hydrostatic pressure, and overpressure are shown in red, green, blue and orange, respectively. Inset shows location where measurements illustrated in the figure were taken.

According to the model, the Lower Cretaceous (100 Ma) source rocks are partially transformed in the western and eastern parts of the basin with greater transformation occurring in the west. While it is 70% transformed in the west (began transformation 75 Ma) (Figure 11a) it is only ca. 10% transformed in the east (Figure 11b). The difference in transformation from west to east is attributed to uplift and folding during the Late Cretaceous, which affected the burial depth and maturation. A similar trend is evident for the Upper Cretaceous (75 Ma) source rock, which is also partially transformed in the west to ca. 50% (began transformation 45 Ma) (Figure 11a), and it has had no transformation in the east (Figure 11b).

The youngest source rock (Eocene-45 Ma) is immature throughout the basin (Figure 11). Immaturity could be caused by inadequate burial. However, it is at an estimated depth of ca. 4 km (13,123 ft), which has resulted in maturity in other regional systems. Source rocks in the Arabian Sub-Basin were mature within 2–4 km (6,561–13,123 ft) of burial (Pollastro, 2003). One cause of the immaturity could be the presence of the Messinian Salt. Salt affects the maturation of hydrocarbons (McBride et al., 1998) and the Messinian Salt is very thick and caused heat loss from the system. The base model from this study shows that the salt dissipated heat through conduction from the system, which contributed to immaturity of the younger source rocks. An alternative model was run that replaced the salt with other lithologies, which had the affect of much greater maturity of the younger source rocks. Since the Messinian Salt is a young deposit it would only affect the youngest source rocks in the system.

Migration patterns are mostly vertical through strata and lateral in carrier beds (Figure 12). The invasion percolation method facilitates vertical movement of fluids across stratal boundaries as well as lateral movement below impermeable strata (Figure 12). Vertical movement of hydrocarbons was

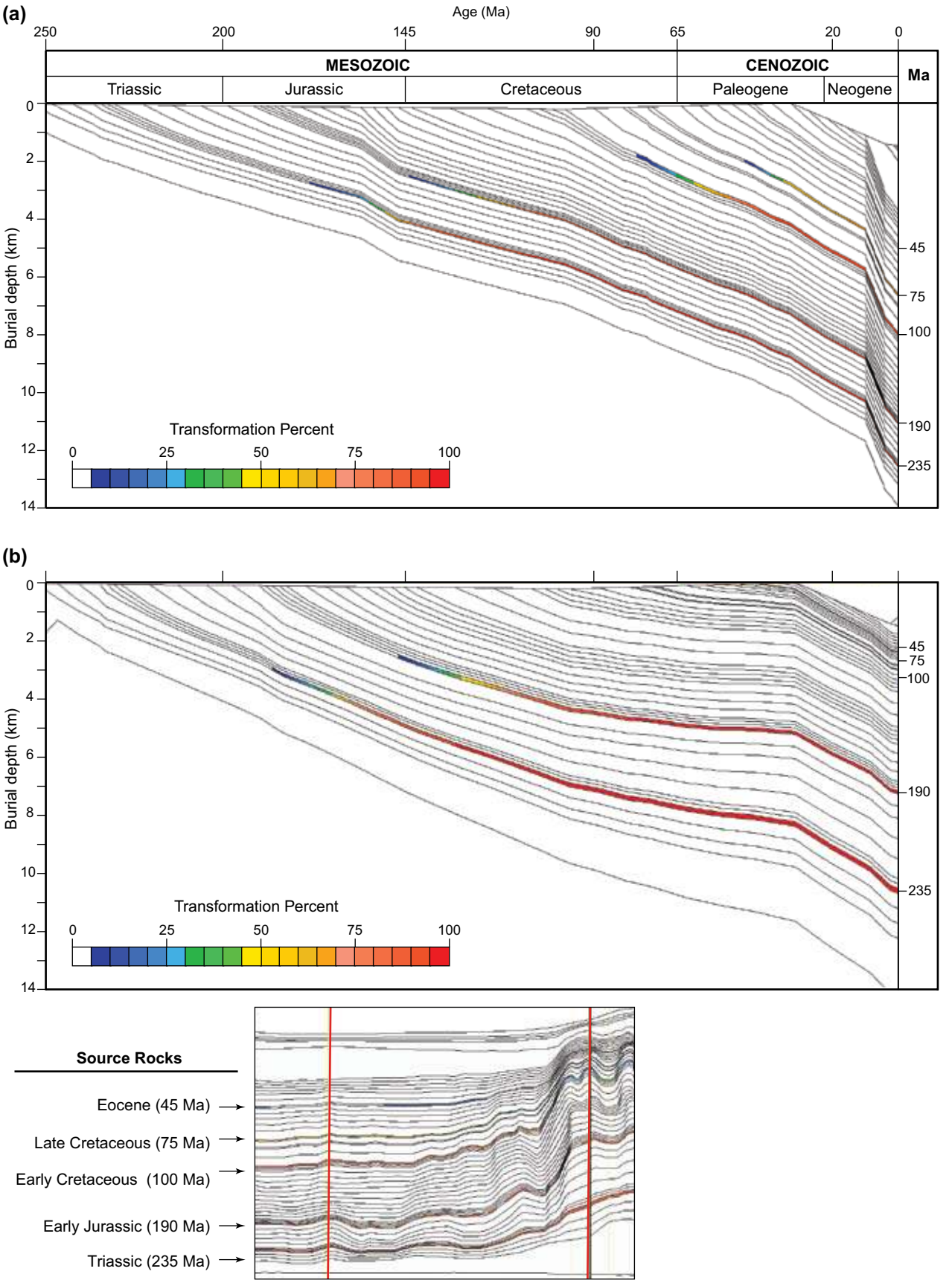

Figure 11: Generation of hydrocarbons from the potential source rocks in the Levantine Basin. The percent of transformation of kerogen to petroleum for the western (a) and eastern (b) parts of the basin are shown. Inset shows location where measurements (a) and (b) illustrated in the figure were taken.

ubiquitous and lateral movement occurred regionally in a west to east direction (downdip to updip), except where folded strata were encountered (Figure 12). The model suggests that hydrocarbons were able to migrate to the structural and stratigraphic traps in the basin (Figure 13b). Most of the accumulations occupy structural traps, primarily folds, and the accumulations are laterally extensive across multiple seismic lines. The sub-Messinian gas play discovered at the Tamar Well is an example of a hydrocarbon accumulation in folded strata. Accumulations similar to Tamar are predicted by this model. Although structural traps are more prevalent, according to the model, hydrocarbon accumulations also occupy stratigraphic traps including, stratal pinchouts, reefs, and talus slopes adjacent to carbonate platforms (Figures 5 and 13b).

Accumulations also occurred adjacent to the salt diapir interpreted in the northern part of the basin (Figure 4). According to the model, three of the petroleum systems were responsible for most of the hydrocarbons preserved in the basin. The important petroleum systems of the basin are associated with the Lower Jurassic and the Lower and Upper Cretaceous source rocks (Figure 14). The Lower Jurassic petroleum system hydrocarbons were generated between 145–85 Ma and migrated into Lower and Upper Cretaceous strata (Figure 14a).

The accumulations of gas and medium oil are in traps that include folds, stratal pinchouts adjacent to folds, reefs, and talus deposits at depths usually at 8–9 km (26,246–29,527 ft). Trap formation occurred throughout the Early Cretaceous and dominantly as stratigraphic traps. Upper Cretaceous traps are the folds and the stratal pinchouts adjacent to folds. Lower Cretaceous reservoir strata are siliciclastic (bypass deposits) or carbonate (platform facies). Chalks have the reservoir potential in the Upper Cretaceous. Seals for this petroleum system are mud-rich strata interbedded with the reservoir facies (siliciclastic and carbonate).

The Lower Cretaceous petroleum system is still in the generation window, however as previously discussed, the source rock in the western part of the basin is 70 percent transformed. These hydrocarbons (medium oil and gas) occupy Upper Cretaceous and Paleogene strata at depths between 6.5–8 km (21,325–26,246 ft) (Figure 14b). The traps are primarily folds. The folds began formation in the Late Cretaceous and continued throughout the Paleogene. Aside from the folds there are also stratal pinchouts against structure in the Upper Cretaceous and Paleogene and stratal pinchouts associated with turbidite deposits in the Paleogene. Primary reservoir rocks for this system are the Upper Cretaceous chalks and siliciclastics from turbidites in the Paleogene. Potential seals are marls interbedded with chalks and muddy siliciclastics within turbidite deposits.

The Upper Cretaceous petroleum system is also still in the generation window but the source rock is 50 percent transformed in most of the basin. The accumulations of medium oil and gas are in folded Paleogene aged at depths from 4.0–5.5 km (13,123–18,044 ft) (Figure 14c). The reservoirs are probably siliciclastic turbidite deposits that are capped by either muddy strata within the turbidites and/or the Messinian Salt.

RISK ANALYSIS

Confidence in the models was assessed by two different methods, multiple scenarios and risking. Comparisons between the results of the base model and results of other scenarios that have different input parameter values suggest that heat flow, thickness of source rock, TOC percent, and lithologic properties affected the volume of hydrocarbons preserved the most. In all cases except the thickness of source rock, TOC percent, and lithologic properties there was more accumulation in reservoirs than with the base model. Thinner source rock and lower percentage of TOC did result in the generation of hydrocarbons, but it was less volume than with the base model and less hydrocarbons accumulated in reservoirs. This result was expected given the correlation between richness and volume of source rock to volume of hydrocarbons produced. Lithologic properties had the same hydrocarbon generation volume in both the base model and the alternative models; however, changes in the anisotropy and lithofacies within the system affected the migration and resulted in less hydrocarbons preserved. Heat-flow variations in all of the models resulted in more hydrocarbons preserved in reservoirs when compared to the base model. In some cases, hydrocarbon generation was less than in the base model (likely due to inadequate heat), but there were less hydrocarbons lost (probably due to less

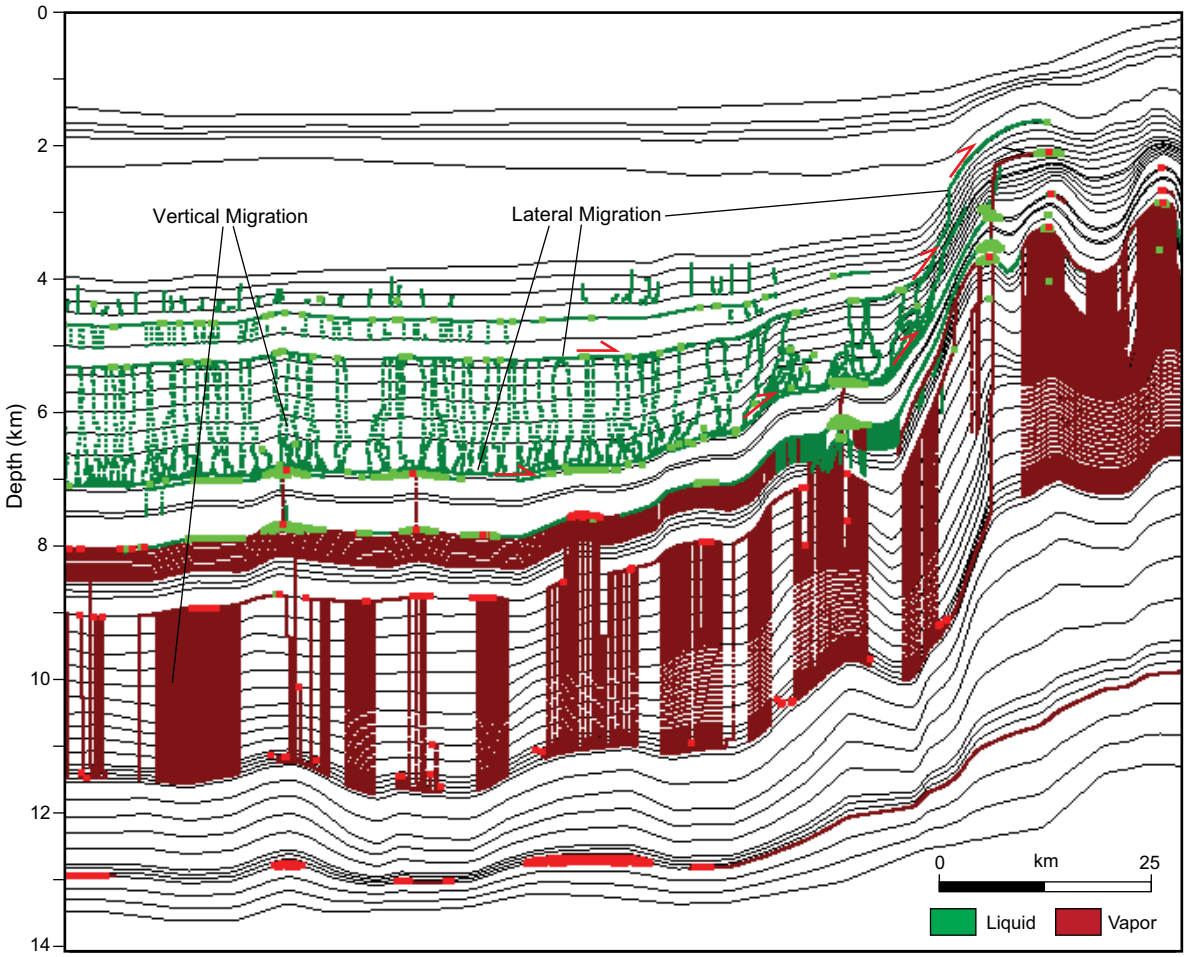

Figure 12: Migration of hydrocarbons throughout the basin; vertical and lateral migration occurred.

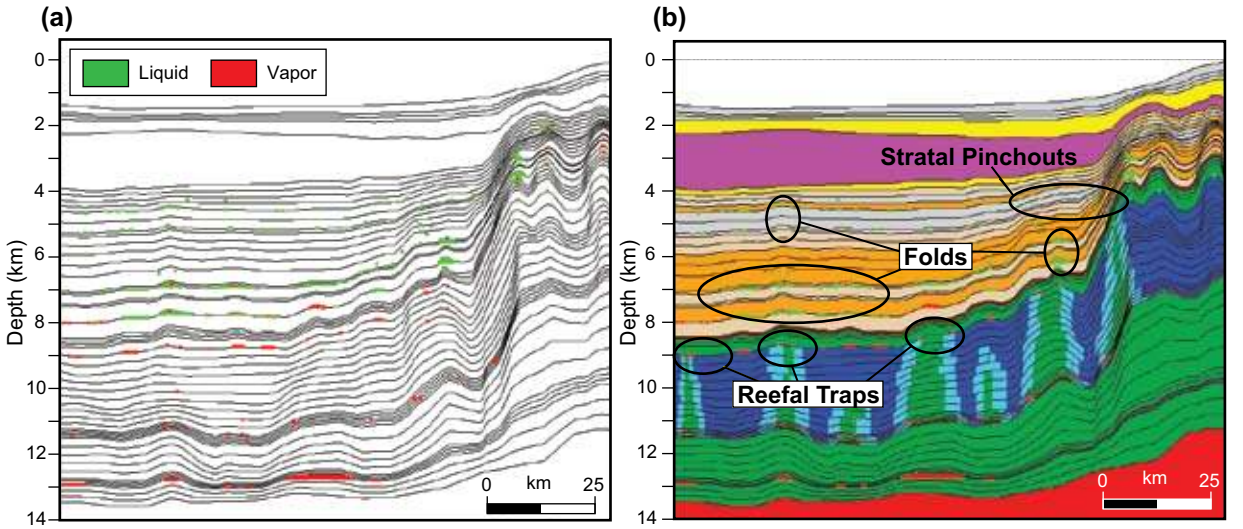

Figure 13: Hydrocarbon accumulations. (a) Illustrates the spatial distribution of oil and gas accumulations. (b) Accumulations occupy potential structural and stratigraphic traps throughout the basin; folds, stratal pinchouts, and reefal traps.

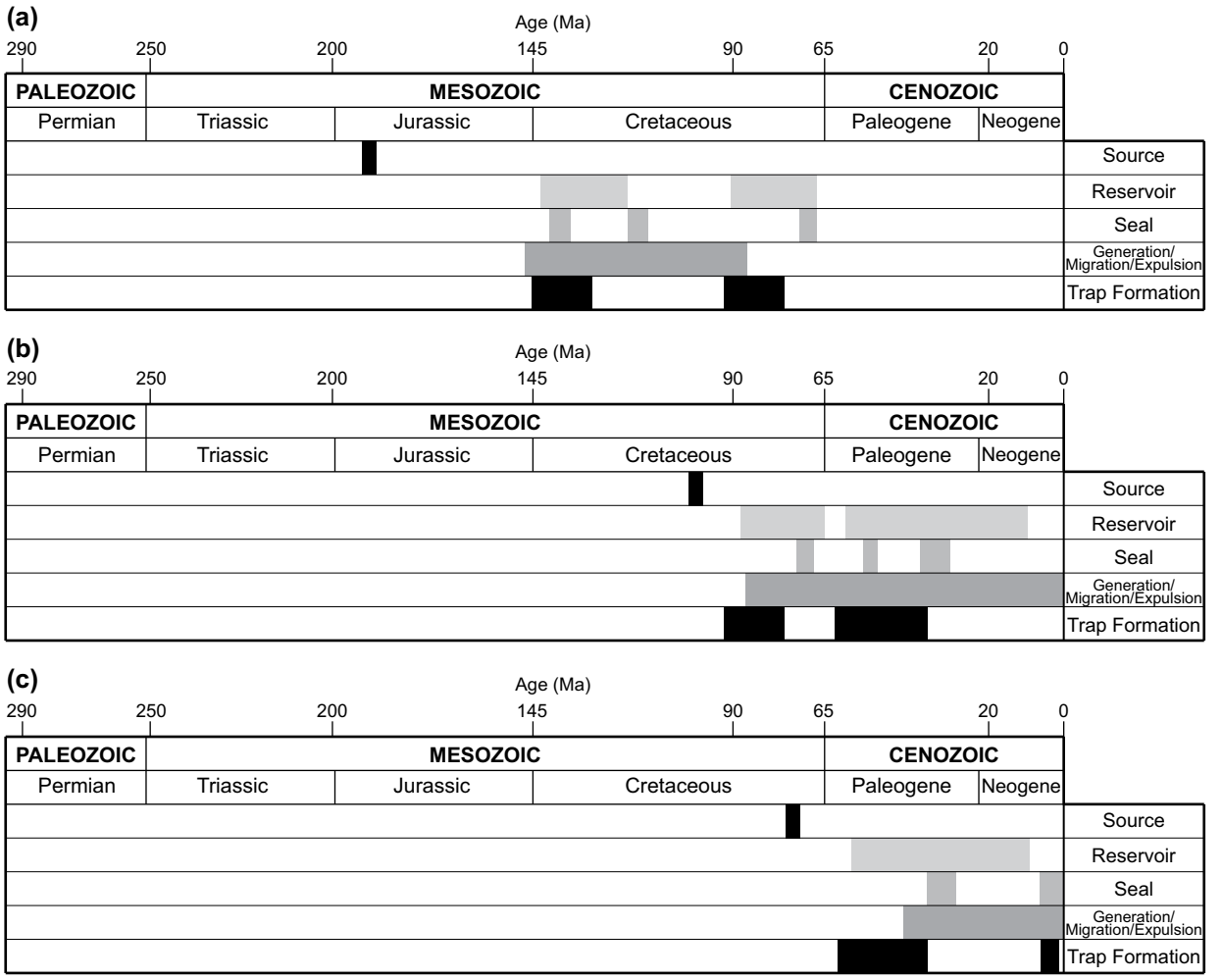

Figure 14: Petroleum system event chart shows the relative timing of generation-migration and trap formation for the designated source rocks in the Levantine Basin: (a) Lower Jurassic (190 Ma); (b) Lower Cretaceous (100 Ma); and (c) Upper Cretaceous (75 Ma).

overcooking) and so the result was that more hydrocarbons were preserved. In other cases with higher heat flow, there were more hydrocarbons generated but there were also more lost, however the resultant hydrocarbon volume preserved was still greater than that in the base model.

Risk analysis results showed that hydrocarbon accumulations are most negatively affected by decreases in heat flow. Heat flow and TOC percentages for all five source rocks in the model underwent Monte Carlo simulation, whereby 50 runs were performed and in each run a different value within a specified range of values was randomly chosen. The specified range of heat flow values used in the risk runs were + 12 wM/m^2 of the original values chosen (Figure 7) from 270 to 5 Ma. Ranges of TOC values used in the simulation were different for each source rock, but the combined range of values for all source rocks was between 0.7 and 4.63 TOC percent. The affect of heat flow and TOC changes on the reservoir accumulation was examined. The greatest correlation was between reservoir accumulation and heat flow. There was less but still positive correlation with the TOC of the source rocks and accumulation. For many of the reservoirs there was greater than 50 percent probability that the reservoir would have the same or greater volume of hydrocarbons, given changes in input values, than the amount predicted by the base model. A decreased volume of hydrocarbons was almost always caused by inadequate heat flow, i.e. a lower value of heat flow relative to the base model values. In several runs a decreased heat flow coupled with increases in TOC still resulted in less accumulation.

CONCLUSIONS

Recent hydrocarbon discoveries in the Levantine Basin confirm the petroleum potential. The Tamar (ca. 5 TCF) and the Dalit gas discoveries along with other numerous shows in Mesozoic and Cenozoic strata near the modern continental slope reinforce the existence of at least one effective source rock. However, given regional analogs of source rocks and the basin's evolution along the Neo-Tethys Ocean there are likely several productive source rocks. The proven petroleum together with the results from this tectono-stratigraphic assessment and 2-D modeling study provide a conceptual framework for future exploration plays. The results of the seismic interpretation together with the 2-D modeling suggest petroleum charge occurred, possibly from multiple source rocks, and there are several candidate seal and reservoir rocks throughout the Phanerozoic stratal package (Figure 14). While the youngest source rocks are immature, most of the source rocks are mature (Figure 11). The timing of transformation, expulsion, and migration was conducive to preservation of hydrocarbons in multiple aged reservoirs (Figures 12, 13 and 14). Moreover, the tectono-stratigraphic history facilitated the formation of many structural and stratigraphic traps throughout the basin (Figures 1 and 13), which could contain oil and gas accumulations (Figure 13). Analysis of uncertainties reinforce confidence in the model results and suggest that even with reasonable variations to the heat flow and other critical parameters, hydrocarbon preservation and accumulation has occurred.

ACKNOWLEDGEMENTS

We thank TGS-NOPEC Geophysical Company (Houston, Texas) for use of the quality seismic and well data used to make the interpretations. We are also grateful to Schlumberger for use of their petroleum systems modeling software, PetroMod2D®. We also thank GeoArabia Designer Nestor "Niño" Buhay IV for designing the manuscript.

REFERENCES

Aal, A.A., A. El Barkooky, M. Gerrits, H. Meyer, M. Schwander and H. Zaki 2000. Tectonic evolution of the Eastern Mediterranean basin and its significance for hydrocarbon prospectivity in the ultradeepwater of the Nile Delta. The Leading Edge, October, p. 1086-1102.

Abdel-Rahman, A.F.M., and F.H. Nader, 2002. Characterization of the Lebanese Jurassic-Cretaceous carbonate stratigraphic sequence: a geochemical approach. Geological Journal, v. 37, no. 1, p. 69-91.

Allen, P.A. and J.R. Allen, 2005. Basin Analysis: Principles and Applications. Blackwell Publishing, 549 pp.

Ben-Avraham, Z., A. Ginzburg, J. Makris, and L. Eppelbaum 2002. Crustal structure of the Levant basin, Eastern Mediterranean. Tectonophysics, v. 346, p. 23-43.

Ben-David, C. 2010. Noble says tests show Leviathan is significant gas discovery off Israel: Bloomberg, Dec 29, http://www.bloomberg.com

Bertoni, C. and J.A. Cartwright 2006. Controls on the basinwide architecture of late Miocene (Messinian) evaporites on the Levant margin (Eastern Mediterranean). Sedimentary Geology, v. 188-189, p. 93-114.

Beydoun, Z.R. 1993. Evolution of the northeastern Arabian plate margin and shelf: Hydrocarbon habitat and conceptual future potential. Revue de l'Institut Francais du Petrole, v. 48, no. 4, p. 311-345.

Beydoun, Z.R. 1999. Evolution and development of the Levant (Dead Sea Rift) transform system: a historical-chronological review of a structural controversy. In C. MacNiocaill and P.D. Ryan (Eds.), Continental Tectonics. Geological Society, London, Special Publication 164. Geological Society of London, London, p. 239-255.

Beydoun, Z.R., and J.G. Habib 1995. Lebanon revisited: New insights into Triassic hydrocarbon prospects. Journal of Petroleum Geology, v. 18, no. 1, p. 75-90.

Bosellini, A. 2004. The western passive margin of Adria and its carbonate platforms. In V. Crescenti, S. D'Offizi, S. Merlino, and L. Sacchi (Eds.), Geology of Italy, Special Volume of the Italian Geological Society for the IGC 32 Florence-2004. Italian Geological Society, Rome, p. 79-92.

Buchbinder, B., and E. Zilberman 1997. Sequence stratigraphy of Miocene-Pliocene carbonate-siliciclastic shelf deposits in the eastern Mediterranean margin (Israel): effects of eustasy and tectonics. Sedimentary Geology, v. 112, p. 7-32.

Dolson, J. C.,M.V. Shann, S. Matbouly, C. Harwood, R. Rashed, and H. Hammouda 2001. The petroleum potential of Egypt. In M.W. Downey, J. C. Threet, and W. A. Morgan (Eds.), Petroleum provinces of the twenty-first century. American Association of Petroleum Geologists Memoir 74, p. 453–482.

Dolson, J.C., P.J. Boucher, J. Siok and P.D. Heppard 2005. Key challenges to realizing full potential in an emerging giant gas province: Nile Delta/Mediterranean offshore, deep water, Egypt. In A.G. Doré and B.A. Vining (Eds.), Petroleum Geology: North-West Europe and Global Perspectives - Proceedings of the 6th Petroleum Geology Conference, 607–624. Petroleum Geology Conferences Ltd. Published by the Geological Society, London.

Druckman, Y., B. Buchbinder, G.M. Martinotti, R. Siman Tov and P. Aharon 1995. The buried Afiq Canyon (eastern Mediterranean, Israel): a case study of a Tertiary submarine canyon exposed in Late Messinian times. Marine Geology, v. 123, p. 167-185.

Eberli , G.P., J.L. Masaferro, and J.F. Sarg (Eds.), 2004. Seismic imaging of carbonate reservoirs and systems. American Association of Petroleum Geologists Memoir 84, 376 pp.

Emery, D., and K.J. Myers 1996. Sequence Stratigraphy. Oxford, Blackwell, 297 pp.

Feinstein, S., Z. Aizenshtat, I. Miloslavski, P. Gerling, J. Slager, and J. McQuilken 2002. Genetic characterization of gas shows in the East Mediterranean offshore of southwestern Israel. Organic Geochemistry, v. 33, p. 1401-1413.

Flexer, A., F. Hirsch, and J.K. Hall 2005. Introduction. In J.K. Hall, V.A. Krasheninnikov, F. Hirsch, C. Benjamini and A. Flexer (Eds.), Geological Framework of the Levant Volume II - The Levantine Basin and Israel: Historical Productions, p. 215-269.

Forrest, M, 2000. 'Bright' investments paid off, www.aapg.org, accessed November 3, 2009 AAPG©2000 reprinted by permission of the AAPG whose permission is required for further use.

Fox, J.E. and T.S. Ahlbrandt 2002. Petroleum geology and total petroleum systems of the Widyan Basin and Interior Platform of Saudi Arabia and Iraq. U.S. Geological Survey Bulletin, v. 2202-E, p. 1-26.

Gardosh, M.A., and Y. Druckman 2006. Seismic stratigraphy, structure and tectonic evolution of the Levantine basin, offshore Israel. In A.H. Robertson and D. Mountrakis (Eds.), Tectonic Development of the Eastern Mediterranean Region. Special Publications 260, Geological Society, London, p. 201-227.

Gardosh, M., Y. Druckman, B. Buchbinder, and M. Rybakov 2008. The Levant Basin Offshore Israel: Stratigraphy, Structure, Tectonic Evolution and Implications for Hydrocarbon Exploration. The Geologic Institute of Israel, 120 pp.

Garfunkel, Z. 1998. Constrains on the origin and history of the Eastern Mediterranean basin. Tectonophysics, v. 298, p. 5-35.

Garfunkel, Z. 2004. Origin of the Eastern Mediterranean basin: a reevaluation. Tectonophysics, v. 391, p. 11-34.

Greitzer, Y. and D. Levitte 2005. Geothermal update report from Israel Proceedings World Geothermal Congress 2005, Antalya, Turkey, 24-29 April 2005, p. 197-199.

Guiraud, R., W. Bosworth, J. Thierry, and A. Delplanque 2005. Phanerozoic geological evolution of Northern and Central Africa: An Overview. Journal of African Earth Sciences, v. 43, p. 83–143.

Hansom, J. and M.K. Lee 2005. Effects of hydrocarbon generation, basal heat and sediment compaction on overpressure development: a numerical study. Petroleum Geoscience, v. 11, p. 353-360.

Hantschel, T. and A.I. Kauerauf, 2009. Fundamentals of Basin and Petroleum Systems Modeling. Springer, 476 p.

Harrison, W.E., K.V. Luza, M.L Prater, and P.K. Chueng 1983. Geothermal resource assessment of Oklahoma, Special Publication 83-1. Oklahoma Geological Survey, 42 p.

Hirsch, F. 2005. Introduction to the stratigraphy of Israel. In J.K. Hall, V.A. Krasheninnikov, F. Hirsch, C. Benjamini, and A. Flexer (Eds.), Geological Framework of the Levant. Volume II-The Levantine Basin and Israel: Historical Productions-Hall, Israel, p. 269-282.

Horscroft, T.R., and J.M. Peck 2005. 'Bottom up' analysis identifies eastern Mediterranean prospects. Offshore Magazine, v. 65, no. 6.

Hsu, K.J., L. Montadert, D. Bernoulli, M.B. Cita, A. Erickson, R.E. Garrison, F. Kidd, R.B. Melieres, C. Muller, and R. Wright 1977. History of the Mediterranean salinity crisis. Nature, v. 267, p. 399-403.

Hubscher, C., J. Cartwright, H. Cypionka, G.J. De Lange, J. Robertson, P. Suc, and J.L. Urai, 2007. Global Look at Salt Giants. EOS, v. 88, no. 16, p. 177-179.

Kendall, C.G., B. Bowen, A. Alsharhan, D. Cheong, and D. Stoudt, 1991. Eustatic controls on carbonate facies in reservoirs and seals associated with Mesozoic hydrocarbon fields of the Arabian Gulf and the Gulf of Mexico. Marine Geology, v. 102, p. 215-238.

Lukasik, J. and J.A. Simo 2008. Controls on carbonate platform and reef development. Society of Economic Paleontologists and Mineralogists, Special Publication, v. 89, Tulsa, OK, 364 pp.

Mart, Y., W.B.F. Ryan, and O.V. Lunina 2005. Review of the tectonics of the Levant rift system: the structural significance of oblique continental breakup. Tectonophysics, v. 395, p. 209-232.

May, P.R. 1991. The eastern Mediterranean Mesozoic basin: evolution and oil habitat. American Association of Petroleum Geologists Bulletin Bulletin, v. 75, p. 1215-1232.

McBride, B.C., P. Weimer, and M.G. Rowan 1998. The Effect of Allochthonous Salt on the Petroleum Systems of Northern Green Canyon and Ewing Bank (Offshore Louisiana), Northern Gulf of Mexico. American Association of Petroleum Geologists Bulletin, v. 82, p. 1112.

Mitchum, R.M., Vail, P.R., and Thompson, S. 1977. Seismic stratigraphy and global changes in sea level, Part 2: the depositional sequence as the basic unit for stratigraphic analysis. In C.E. Payton (Ed.), Seismic Stratigraphy: Application to Hydrocarbon Exploration. AAPG Memoir, v. 26, p. 53-62.

Mouty, M. 2000. The Jurassic in Syria: an overview. Lithostratigraphic and biostratigraphic correlations with adjacent areas. In S. Crasquin-Soleau and E. Barrier (Eds.), Peri-Tethys Memoir 5. New Data on Peri-Tethyan Sedimentary Basins. Memoires Museum National d'Histoire Naturelle, v. 182, p. 159-168.

Murris, R.J. 1980. Middle East: stratigraphic evolution and oil habitat. American Association of Petroleum Geologists Bulletin, v. 64, no. 5, p. 597-618.

Nader, F.H. and Swennen, 2004. Petroleum prospects of Lebanon; some remarks from sedimentological and diagenetic studies of Jurassic carbonates. Marine and Petroleum Geology, v. 21, no. 4, p. 427-441.

Netzeband, G.L., K. Gohl, C.P. Hubscher, Z. Ben-Avraham, G.A. Dehghani, D. Gajewski, and P. Liersch 2006. The Levantine basin-crustal structure and origin. Tectonophysics, v. 418, p. 167-188.

Offshore Engineer Staff, 2009. Matan Matters: Offshore Engineer Digest, March 23, http://www.offshore-engineer.com

Offshore staff, 2010. USGS confirms Levantine Basin prospectivity: Offshore, Apr 22, http://www.offshore-mag.com

Peck, J.M. 2008. Giant oil prospects lie in distal portion of offshore East Mediterranean basin. Oil and Gas Journal, Oct. 6, v. 106, p. 41-42, 44-49.

Pepper, A. and P. Corvi 1995. Simple kinetic models of petroleum formation. Part I: oil and gas generation from kerogen. Marine and Petroleum Geology, v. 12, no. 3, p. 291-319.

Pollastro, R.M. 2003. Total Petroleum Systems of the Paleozoic and Jurassic, Greater Ghawar Uplift and Adjoining Provinces of Central Saudi Arabia and Northern Arabian-Persian Gulf. U.S. Geological Survey Bulletin, v. 2202-E, p. 1-100.

Pomar, L. 2001. Types of carbonate platforms, a genetic approach. Basin Research, v. 13, p. 313-334.

Posamentier, H.W. and Allen, G.P. 1999. Siliciclastic sequence stratigraphy – Concepts and applications. Society of Economic Paleontologists and Mineralogists Concepts in Sedimentology and Paleontology, v. 7, 210 pp.

Read, J.F. 1985. Carbonate platform facies models. American Association of Petroleum Geologists Bulletin, v. 69, p. 1-21.

Renouard, G. 1955. Oil prospects of Lebanon. American Association of Petroleum Geologists Bulletin, v. 39. p. 2125-2169.

Roberts, G. and D. Peace 2007. Hydrocarbon plays and prospectivity of the Levantine Basin, offshore Lebanon and Syria from modern seismic data. GeoArabia, vol. 12, no. 3, p. 99-124.

Robertson, A.H.F. 1998. Mesozoic-Tertiary tectonic evolution of the Easternmost Mediterranean area. Integration of marine and Land evidence. In A.H.F. Robertson, C. Richter, and A. Camerlenghi (Eds.), Proceedings of the Ocean Drilling Program, Scientific Results v. 160. Texas A & M, TX, p. 723-782.

Robertson, A.H.F. 2002. Overview of the genesis and emplacement of Mesozoic ophiolites in the Eastern Mediterranean Tethyan region. Lithos, v. 65, p. 1-67.

Robertson, AH.F. and Z. Dixon 1984. Introduction: aspects of geological evolution of the Eastern Mediterranean, In J.E. Dixon and A.H.F. Robertson (Eds.), The Geological Evolution of the Eastern Mediterranean. Blackwell Scientific, Boston, p. 1-71.

Sadooni, F.N. and A.S. Alsharhan 2004. Stratigraphy, lithofacies distribution, and petroleum potential of the Triassic strata of the northern Arabian plate. American Association of Petroleum Geologists Bulletin, v. 88, no. 4, p. 515-538.

Sawaf, T., G. Brew, R. Litak, and M. Barazangi 2001. Geologic evolution of the intraplate Palmyride Basin and Euphrates Fault System, Syria. In P.A. Ziegler et al. (Eds)., Peri-Tethys Memoir 6: Peri-Tethyan Rift/Wrench Basins and Passive Margins. Memoires Museum National d'Histoire Naturelle, v. 186, p. 441-467.

Scandinavian Oil and Gas Magazine Staff 2009. Noble discovers gas at Dalit offshore Israel. Scandinavian Oil and Gas Magazine, March 31 http://www.scandoil.com

Schattner, U., Z. Ben-Avraham, M. Lazar, and C. Huebscher 2006. Tectonic isolation of the Levant basin offshore Galiliee-Lebanon-effects of Dead Sea fault plate boundary on Levant continental margin, Eastern Mediterranean. Journal of Structural Geology, v. 28, p. 2049-2066.

Schlager, W. 2005. Carbonate Sedimentology and Sequence Stratigraphy, Society of Economic Paleontologists and Mineralogists Concepts in Sedimentology and Paleontology 8. Tulsa, OK, 200 pp.

Semb, P.H. 2009. Possible seismic hydrocarbon indicators in offshore Cyprus and Lebanon. GeoArabia, v. 14, no. 2, p. 49-66.

Sharland, P.R., R. Archer, D.M. Casey, R.B. Davies, S.H. Hall, A.P. Heward, A.D. Horbury, and M.D. Simmons 2001. Arabian Plate Sequence Stratigraphy. GeoArabia, Special Publication 2, Bahrain, 371 pp. and 3 enclosures

Stampfli, G., G. Borel, W. Cavazza, J. Mosar, and P.A. Ziegler (Eds.), 2001. The Paleotectonic Atlas of the PeriTethyan Domain. Berlin, European Geophysical Society.

Swarbrick, R., M. Osborne, and G. Yardley 2002. Comparison of overpressure magnitude resulting from the main generating mechanisms. American Association of Petroleum Geologists Memoir, v. 76, p. 1-12.

Sweeney, J. and A. Burnham 1990. Evaluation of a simple model of vitrinite reflectance based on chemical kinetics. American Association of Petroleum Geologists Bulletin, v. 74, no. 10, p. 1559-1570.

Toland, C. 2000. A sequence stratigraphic reference section for the Tithonian of Lebanon. Society for Sedimentary Geology Special Publication, v. 69, p. 53-64.

Vahrenkamp, V.C., F. David, P. Duijndam, M. Newall, and P. Crevello 2004. Growth architecture, faulting and karstification of a Middle Miocene carbonate platform, Luconia Province, offshore Sarawak, Malaysia. In *G.* Eberli, J.L. Masaferro, and J.F. Sarg (Eds.), Seismic imaging of carbonate reservoirs and systems. American Association of Petroleum Geologists Memoir, v. 84, p. 329-350. AAPG©2004 reprinted by permission of the AAPG whose permission is required for further use.

Vail, P.R., R.M. Mitchum Jr. and S. Thompson III 1977. Seismic stratigraphy and global changes of sea level, part 3: Relative changes of sea level from coastal onlap. In C. Payton (Ed), Seismic Stratigraphy -Applications to Hydrocarbon Exploration. American Association of Petroleum Geologists Memoir, v. 26, p. 63-81.

Waite, L., and R. Gilcrease 2002. Phanerozoic Cycles and Events, Global Stratigraphic Chart. Pioneer Natural Resource, 1 sheet.

Walley, C.D. 1998. Some outstanding issues in the geology of Lebanon and their importance in the tectonic evolution of the Levant region. Tectonophysics. v. 298, p. 37-62.

Walley, C.D. 1997. The lithostratigraphy of Lebanon: A review. Lebanese Science Bulletin, v. 10, no.1, p. 81-108.

Walley, C.D. 2001. The Lebanon passive margin and the evolution of the Levantine Neothethys. In P.A. Ziegler, A.H.F. Robertson, and S. Crasquin-Soleau (Eds.), Peri-Tethys Memoir 6: Peri-Tethyan Rift/Wrench Basins and Passive Margins. Memoires Museum National d'Histoire Naturelle, v. 186, p. 407-439.

Weissbrod, T., 2005. The Paleozoic in Israel and Environs. In J.K. Hall, V.A. Krasheninnikov, F. Hirsch, C. Benjamini, and A. Flexer (Eds.), Geological Framework of the Levant, Volume II: The Levantine Basin and Israel. Historical Productions, Israel, p. 283-316.

Ziegler, P.A., W. Cavazza, A.H.F. Robertson, and S. Crasquin-Soleau (Eds.) 2001. Peri-Tethys Memoir 6: Peri-Tethyan Rift/Wrench Basins and Passive Margins. Memoires Museum National d'Histoire Naturelle, v. 86, 762 pp.

ABOUT THE AUTHORS

Lisa Marlow *is an Exploration Geologist at Shell and also a PhD candidate at the University of Minnesota, USA. Her PhD work involved determining the tectonic and depositional history and petroleum potential of the Levantine Basin using 2-D seismic and well data (TGS NOPEC) and analyzing the petroleum systems in the basin using 2-D modeling software PetroMod2D). Lisa has her MSc from the University of Minnesota where she specialized in glacial geology and post-glacial aeolian deposits.*

Lisa.Marlow@shell.com

Kristijan Kornpihl *is a EAF Project Supervisor Petroleum Systems Modeling WesternGeco Geosolutions Schlumberger, Aachen. He has worked as a Basin and Petroleum Systems modeler with the PetroMod software for the last six years. Kristijan has been part of the PetroMod team at Schlumberger. Prior to Schlumberger's acquisition of IES he was with IES for three years. He received his doctorate in Natural Sciences from Rheinische Friedrich Wilhelms University of Bonn (Germany) where he worked on tectono-sedimentary basin analysis. He obtained his Diploma in Geology and Palaeontology from the University of Cologne, Germany.*

kkornpihl@slb.com

Christopher G. St. C. Kendall *is a Distinguished Emeritus Professor of the University of South Carolina, USA. He is an expert on sequence stratigraphy and consults in exploration and reservoir sedimentology and petrology. Christopher is currently a consultant for Schulumberger studying the Mesozoic carbonate systems of Kuwait.*

kendall@scarolina.edu

Manuscript received August 20, 2010

Revised October 11, 2010

Accepted October 13, 2010

Press version proofread by authors March 9, 2011